Contents

7. Sensors

1. Non-invasive sensing
2. Flow Sensors
3. Chemical Sensors

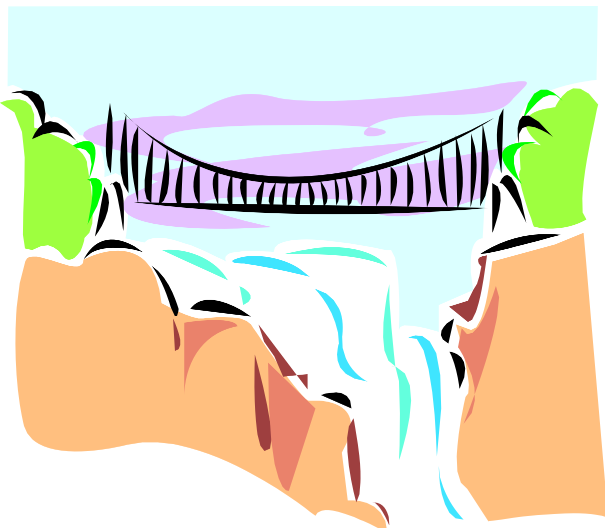

7. Sensors

1. **Non-invasive sensing**
2. Flow Sensors
3. Chemical Sensors

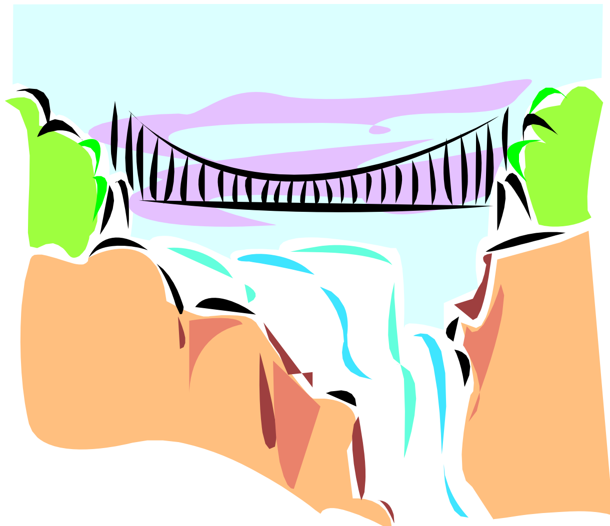

7.1. Macroscopic Methods of Flow Measurement

- Hydrodynamic measurement of **velocity** and volume flow
  - Venturi-nozzle
  - Revolution frequency of turbine

- Particle image velocimetry
  - Non-invasive technique
  - Particle moving with fluid
  - Frequency shift of laser light reflected by moving particles
  - For transparent media
  - Ultrasound may be used if lower precision acceptable

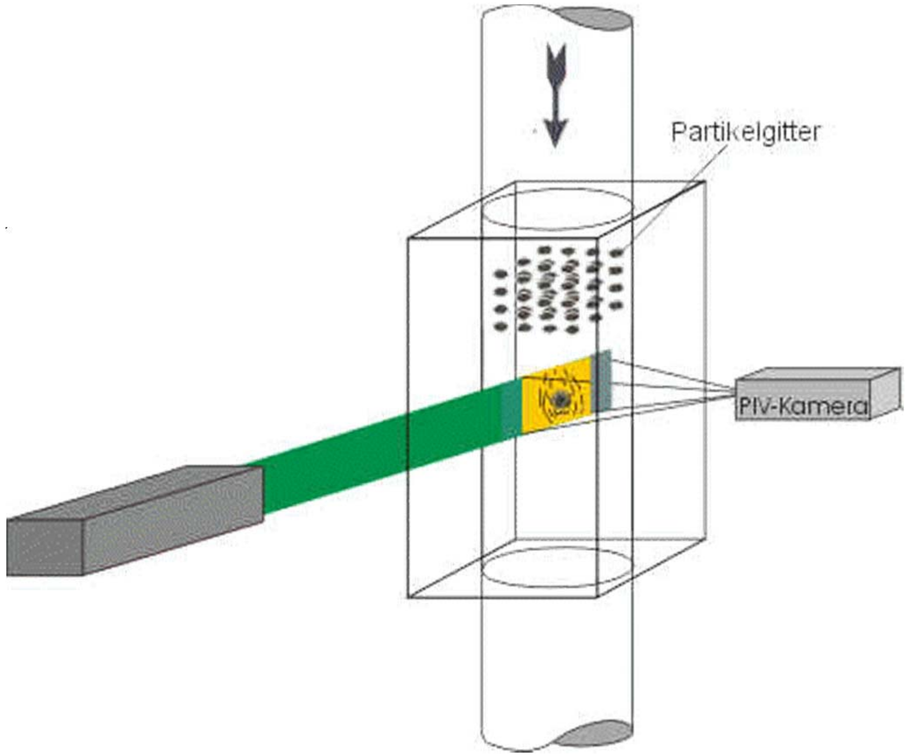

7.1. µ-Particle Image Velocimetry (µPIV)

- Measurement of **flow fields** in µ-scale fluidic devices
- Epi-fluorescent microscope
- 100 to 300 nm seed particles
- Modes for calculation of velocity vector fields
  - Instantaneous (e.g. laser or acoustic Doppler shift)
  - Double frame + cross-correlation algorithm
- Intensified CCD camera for capturing high-resolution particle-image fields
- Limiting factors for spatial resolution and accuracy
  - Diffraction limit of recording optics
  - Noise in particle image field
  - Interaction of fluid with finite-size seed particles
  - Precision of instantaneous velocity measurements
    - Dependent on stochastic Brownian motion

7.1. Molecular Tagging Velocimetry

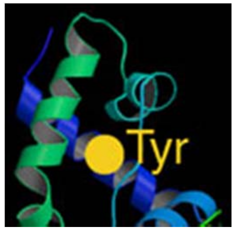

- Time-of-flight (ToF) technique
- Laser writes mark (e.g. a line) into flow
  - By optical resonance with suitable target tracer molecule
- Measurement in gas phase
  - E.g. high-vapor-pressure molecule like acetone merged with fluid
- Upon absorption of laser photon by tracer molecules
  - Relatively long-lived radiative emission
- Recording of line in shot delayed with respect to initial excitation
- Spatially resolved velocity profile by image processing

7. Sensors

1. Non-invasive sensing
2. **Flow Sensors**
3. Chemical Sensors

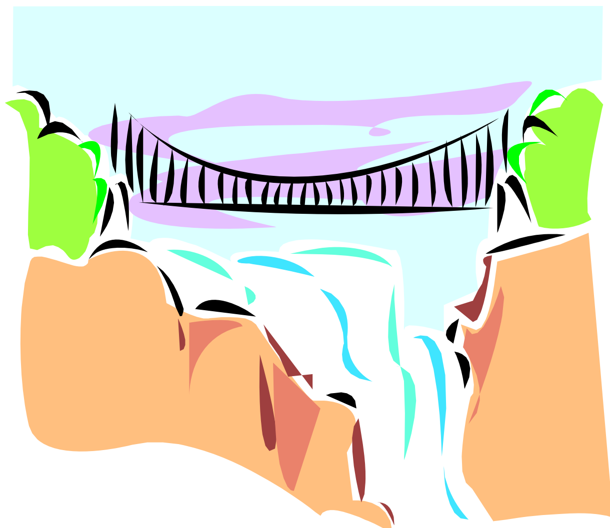

7.2. Flow Sensors

- Measurement of (overall) flow rate
- Main branch of field of sensors
- New technological options for microsensors
  - Novel measurement principles
    - Micro-calorimetry
    - Time-of-flight for thermal signals
  - Novel thermal insulation principles
    - Si-bridges and cantilever
    - Membranes or bridges made of insulating Si_3N_4
  - Short thermal response times
    - Low thermal masses
  - Compact size
    - (Reduced pressure drop)
  - Fabrication by microtechnology
- Potential for
  - Cost reduction
  - Enhanced performance
  - Novel fields of application
    - E.g. microdosage systems

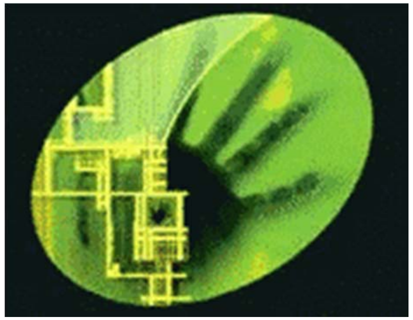

7.2. Classification by Measurement Method

- Mechanical
  - Principle: force or torque
  - Deflection of cantilever
  - Torsion of flow channel by Coriolis force
- Static pressure
  - Differential measurement of pressure
  - Measurement of high flow rates
- Thermal
  - Principle: transfer of thermal energy
  - Heaters and thermometer
  - Thermally insulated
  - Suitable for microfabrication
  - For measurement of minute flow rates
- Direct velocity measurement
  - Time intervals of suspended particles
  - Laser-Doppler-Anemometry (LDA)

7.2. Transduction of Output Signals

- Piezo-resistive
  - Suitable for microfabrication
  - Measurement e.g. by Wheatstone bridge
  - Most frequent technique for micro flow sensors
- Capacitive
- Frequency-analogue

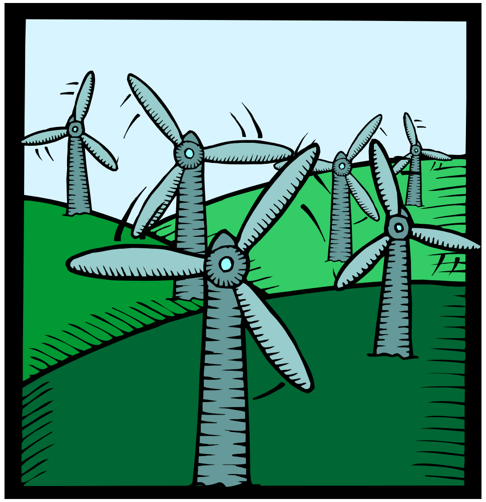

7.2. Flow Sensors

1. Physical Sensor Components
2. Drag-Force Flow Sensors
3. Differential Pressure Flow Sensors
4. Thermal Flow Sensors
5. EHD Mass Flow Sensors
6. Coriolis Mass Flow and Density Sensor
7. Meniscus Detection

7.2.1. Physical Sensor Components

- Pressure sensors
  - Membrane
  - Piezo-resistive transducer

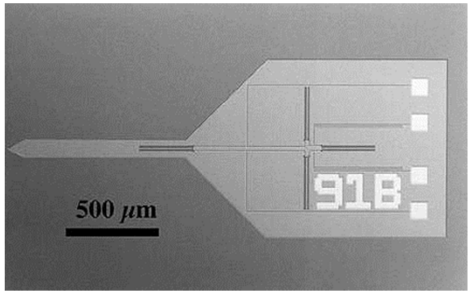

- Temperature sensors
  - Thermopile
  - *T*-dependent resistance

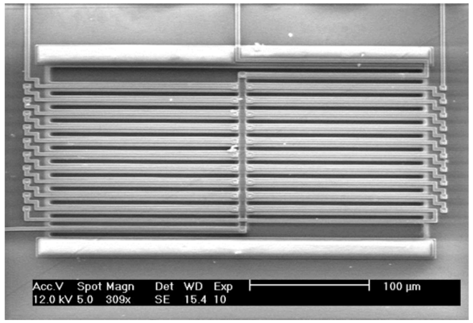

Important issue:
Contact between liquid and sensor material!

7.2. Flow Sensors

1. Physical Sensor Components
2. Drag-Force Flow Sensors
3. Differential Pressure Flow Sensors
4. Thermal Flow Sensors
5. EHD Mass Flow Sensors
6. Coriolis Mass Flow and Density Sensor
7. Meniscus Detection

7.2.2. Mechanical Cantilever-Flow Sensor

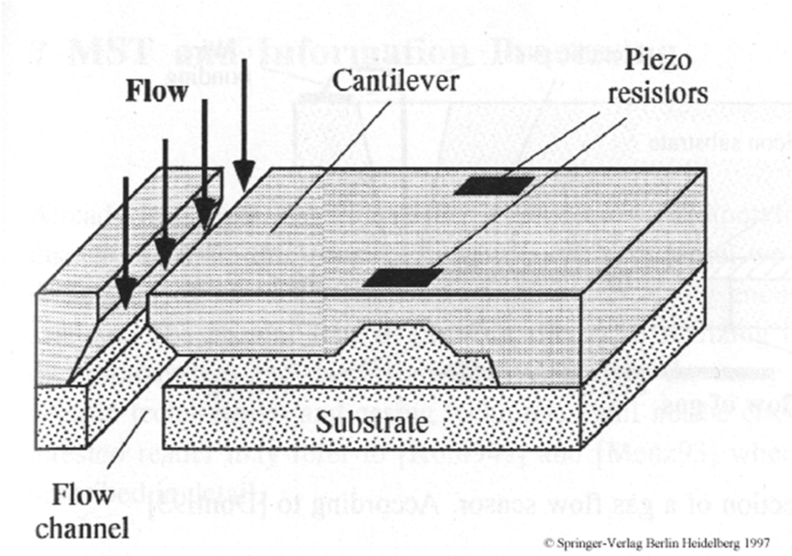

- Cantilever with integrated piezo-resistor
  - Deflection of cantilever by flow
  - Change of piezo-resistance and output signal (voltage)
- Dimensions of cantilever: 3 mm (length), 1 mm (width), 30 µm (thickness)
- Fabrication by surface and bulk micromachining
- Operating range: 5 ml / min to 500 ml / min
- Sensitivity: 4.4 µV / V per µl / min

7.2.2. Drag-Force Flow Sensors

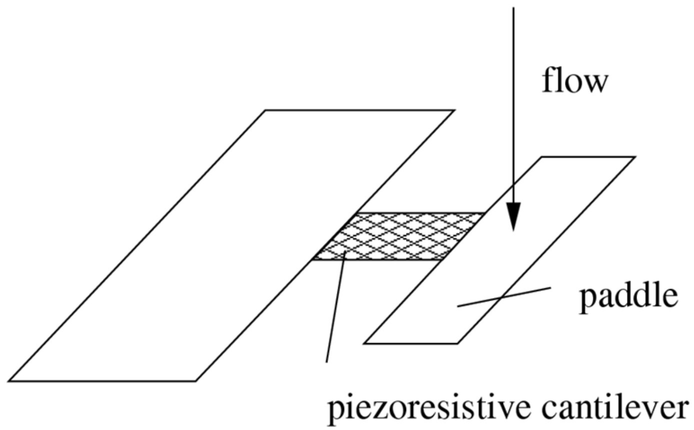

Fig. 7.1. The flow velocity relates to the hydrodynamic drag which is exerted by the flow on the paddle. A piezo-electric transducer on the converts the mechanical stress on the cantilever beam into an electric resistance signal

- Piezo-resistive cantilever
- Deflection of paddle
  - Hydrodynamic force
  - Laminar
    - Deflection linear in *v*
  - Turbulent
    - Deflection with square of *v*

7.2. Flow Sensors

1. Physical Sensor Components
2. Drag-Force Flow Sensors
3. Differential Pressure Flow Sensors
4. Thermal Flow Sensors
5. EHD Mass Flow Sensors
6. Coriolis Mass Flow and Density Sensor
7. Meniscus Detection

7.2.3. Dynamic and Static Pressure

- Horizontal flow at velocity *v* (no gravity)

$$p_{ges} = p + \frac{\rho}{2} v^2 = const.$$

- Liquid at rest:

$$v = 0 \Rightarrow p = p_{ges}$$

- Static pressure *p*:
  - ➢ Pressure sensor moving with fluid
  - ➢ Measurement: Surface of sensor **parallel** to flow vector *v*
- Total pressure p_{ges}:
  - ➢ Measurement: Surface of sensor **perpendicular** to flow vector *v*
  - ➢ Pitot tube (Henri de Pitot, 1695-1771)

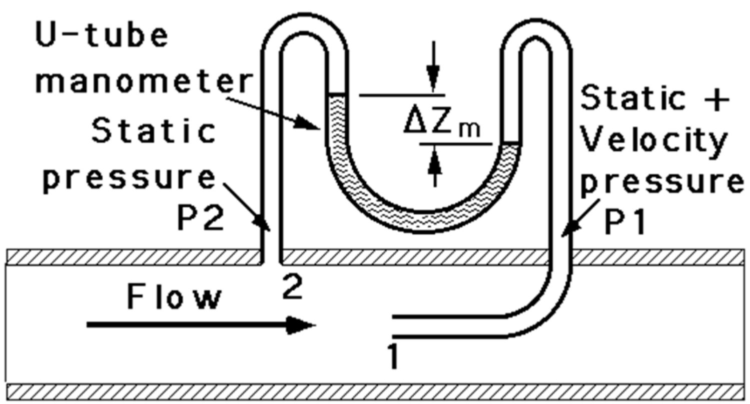

7.2.3. Measurement of Flow Velocity

- Dynamic Pressure
  - Adds to static pressure
  - Differential measurement
  - Prandtl tube

$$\frac{\rho}{2}v^2 = p_{\text{ges}} - p$$

- Real
  - Turbulences
  - Pressure drop at sensor head
  - Device-specific correction factor c_0
- Transformation of Bernoulli equation

$$v = \sqrt{\frac{2(p_{\text{ges}} - p)}{\rho}}$$

- *v* proportional to square root of dynamic pressure
  - Drawback: low sensitivity at small *v*

7.2.3. Venturi Nozzle

- Giovanni B. Venturi (1746-1822)
- Contraction of channel
  - Hydrodynamic pressure drop limit flow
  - Shape of nozzle may alter in long-term experiments

$$p + \frac{\rho}{2} v^2 = p_0 + \frac{\rho}{2} {v_0}^2 = p_{ges} = const.$$

$$Av = A_0 v_0 = const.$$

$$v = \sqrt{\frac{2(p - p_0)}{\rho\left(A^2 / {A_0}^2 - 1\right)}}$$

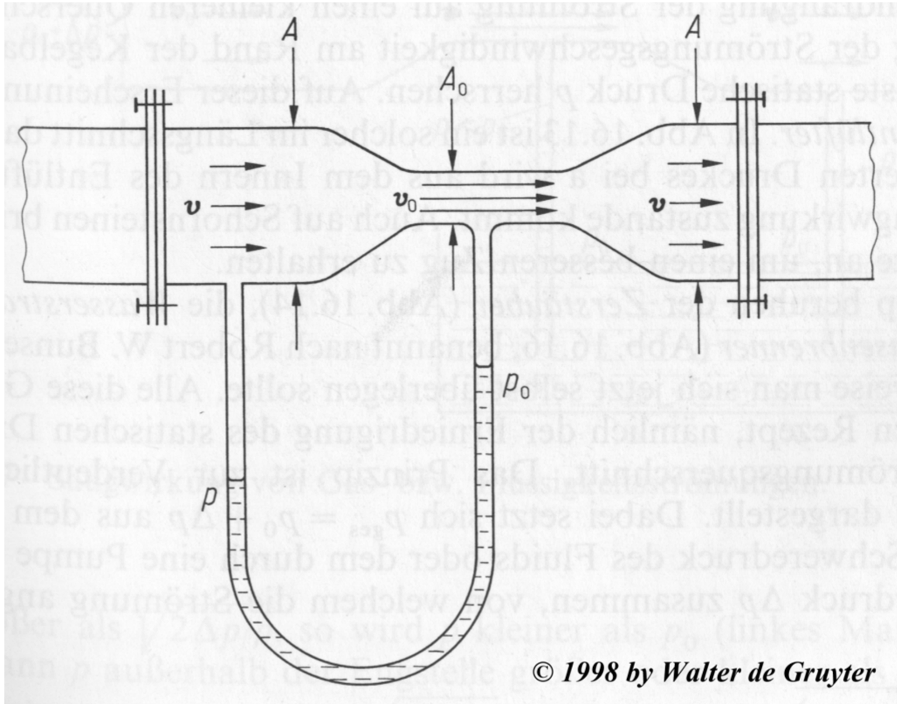

7.2.3. Differential Pressure Sensor - Setup

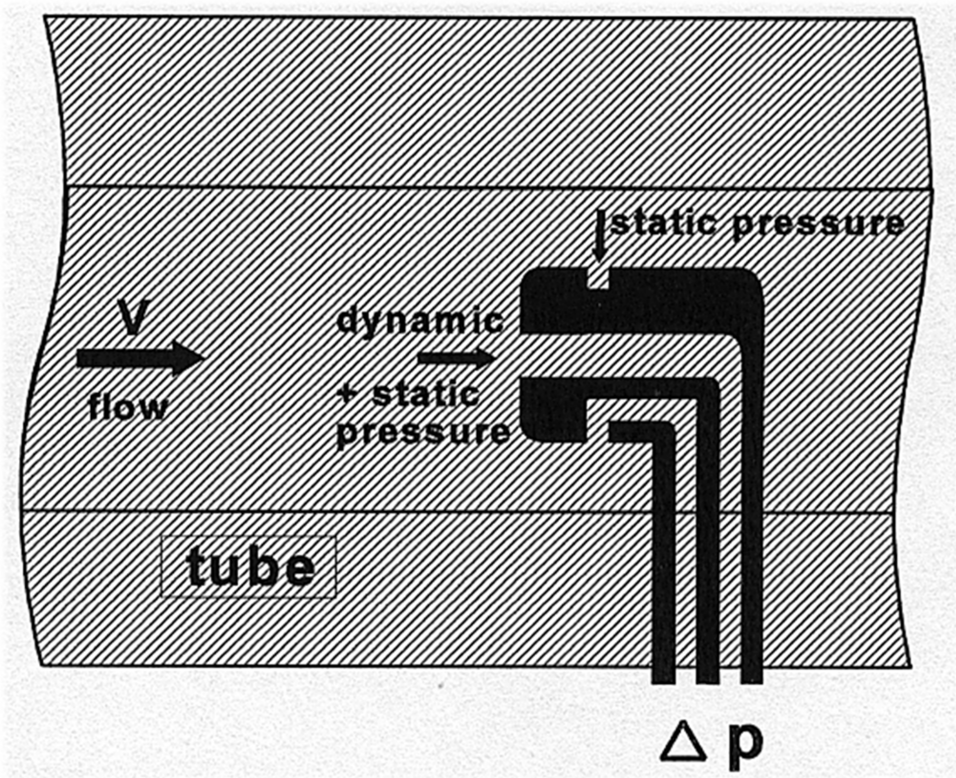

- Prandtl tube
- **External** differential pressure sensor Δ*p*

7.2.3. Micro-Differential Pressure Sensor

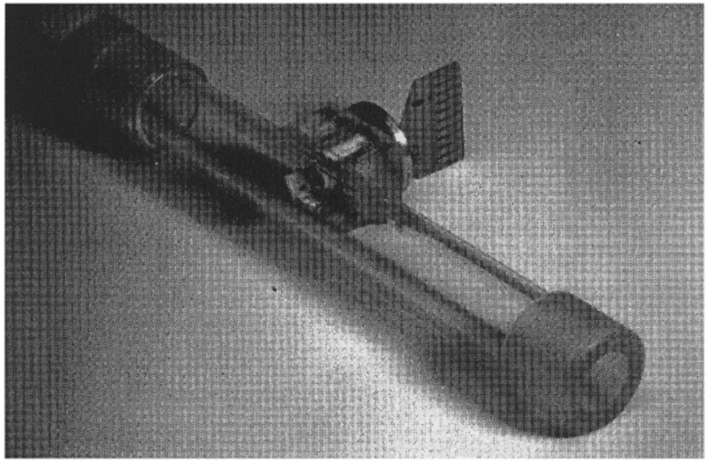

- Flow measurement of **non-aggressive liquids** like water
- Application: fresh and hot water consumption in household
- Low cost fabrication
- High production numbers
- Injection molded housing
- Overall dimensions on cm-scale
- Sensor element: Ø 6 mm, length: 20 mm
- Flow rates up to 5000 l / h
- Pressure measurement within flow, no tubing to exterior

7.2.3. Chip Setup

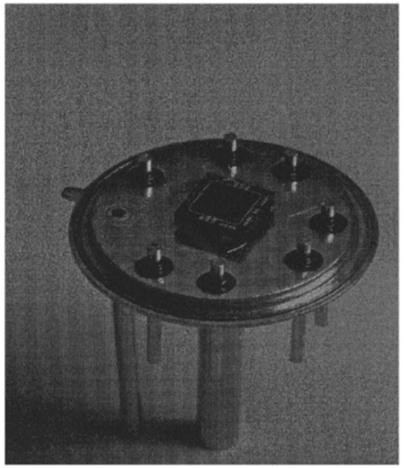

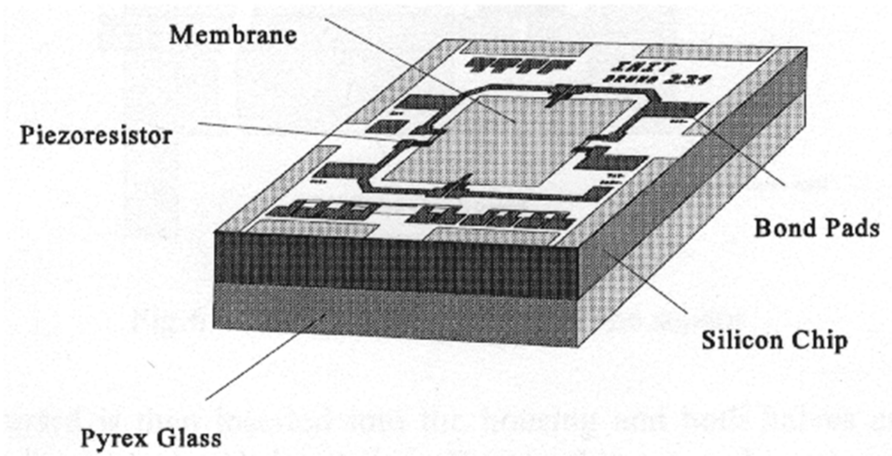

- **Monocrystalline Si-chip** measuring 3 x 3 x 0,5 mm^3
- **Pyrex-substrate**
- **Pressure-membrane etched** with 2 x 2 mm^2 surface and 8 µm thickness
- Differential pressure deflects membrane
- Piezo-resistors pick up mechanical stress (overall resistance: 5 kΩ)
- Measurement by **Wheatstone bridge**
- Transduction of resistance in voltage signal
- Sensitivity 60 µV / hPa

7.2.3. Characteristic Curve

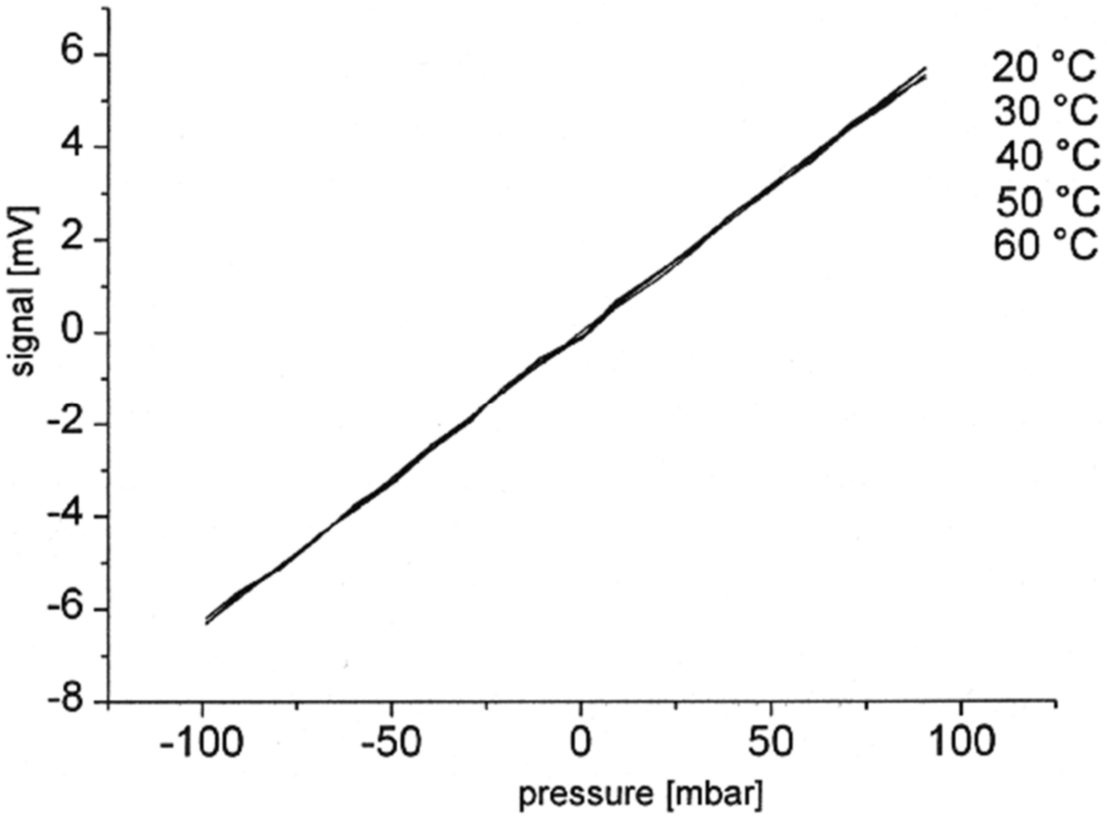

- **Non-Linearity** below 1%
- **Maximum offset** of 20 mV (can be compensated by electronics)
- Low temperature drift

7.2.3. Design of Housing

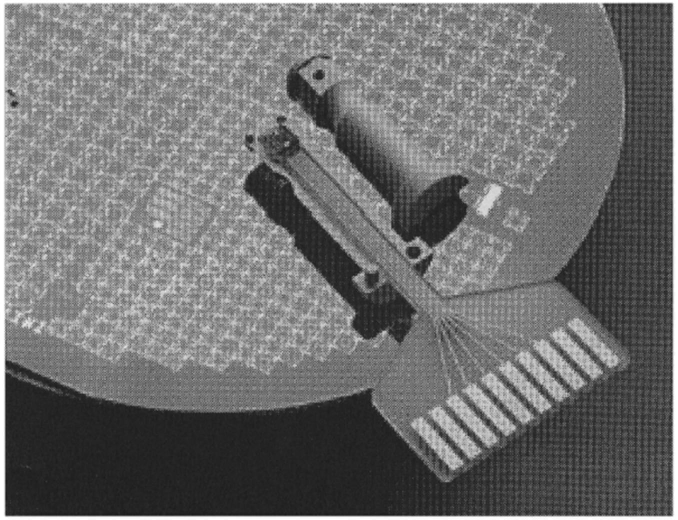

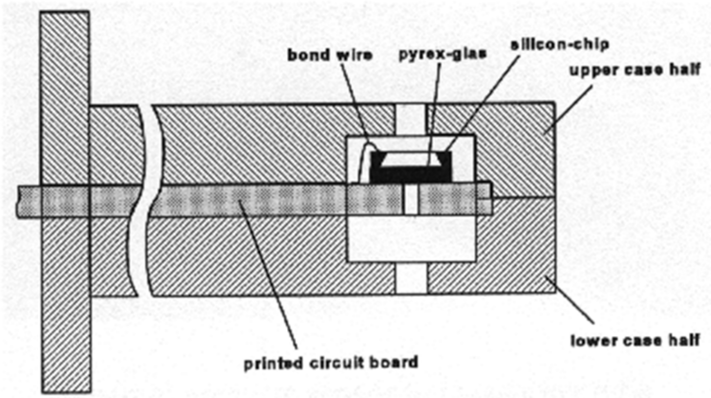

- Protection against turbulence formation and dirt
- Hexagonal housing
  - ➢ Laminar flow without flow separation
- Insulation and feedthrough of electric connections
- Resisting up to 10 bar static pressure
- Low manufacturing costs
- Protected of Si against corrosion by 5-µm Parylene-C layer

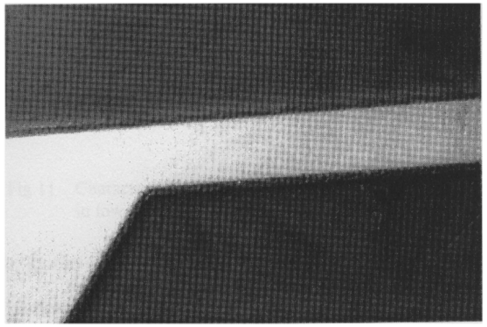

7.2.3. Characteristic Curves

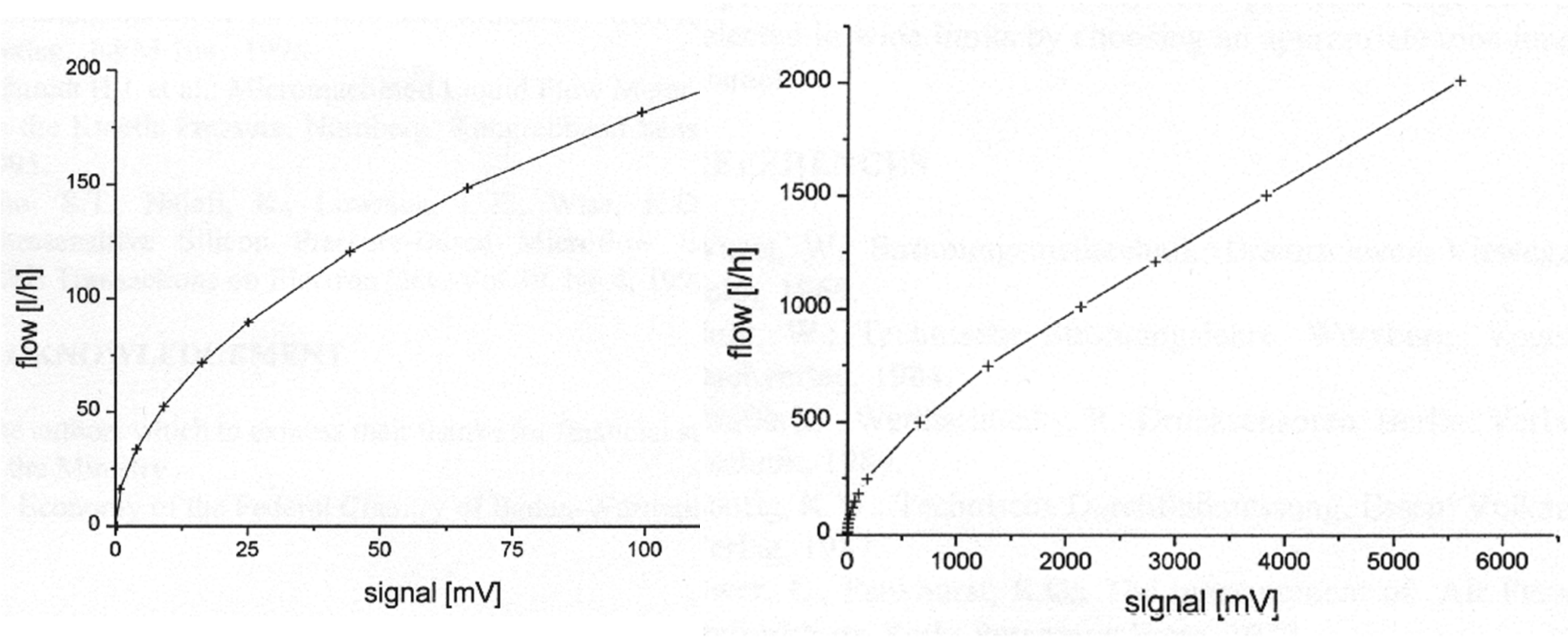

- Read-out electronics
  - Current source for Wheatstone bridge
  - Analogue preamplifier (x 50)
  - AD-converter
  - Microprocessor (storage of characteristic curve)
- Two domains of flow velocities
- Pressure drop at 2500 l / h: 200 hPa, rapidly decreasing towards decreasing *v*

7.2.3. Sensor Performance

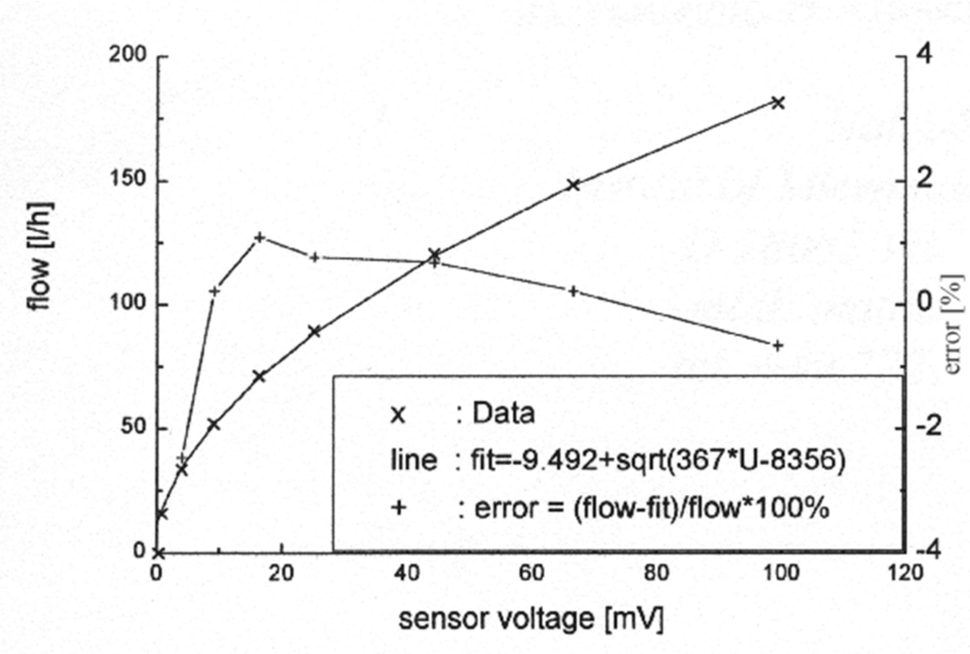

- Measurement error: deviation from fit to square root
- Dynamic band width: 1:50 at
  - Max. 2% deviation form fit
  - Maximum of 200 hPa pressure drop
  - Maximum flow rate 2500 l / h
- Response time 10 ms
- Reliability proven in long-term deployment and mechanical shock

7.2. Flow Sensors

1. Physical Sensor Components
2. Drag-Force Flow Sensors
3. Differential Pressure Flow Sensors
4. Thermal Flow Sensors
5. EHD Mass Flow Sensors
6. Coriolis Mass Flow and Density Sensor
7. Meniscus Detection

7.2.4. Principle of Thermal Conductivity

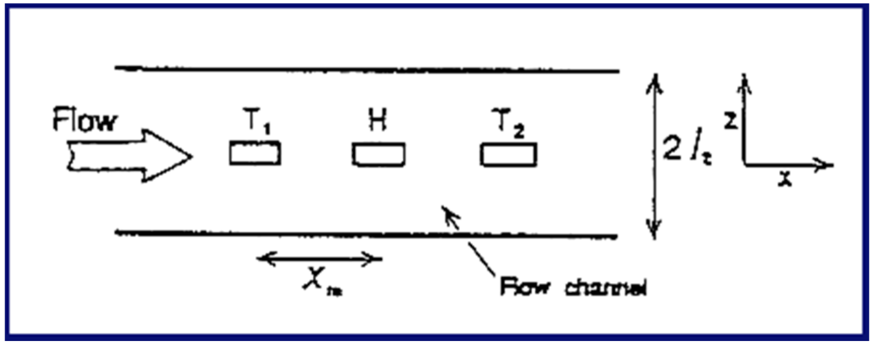

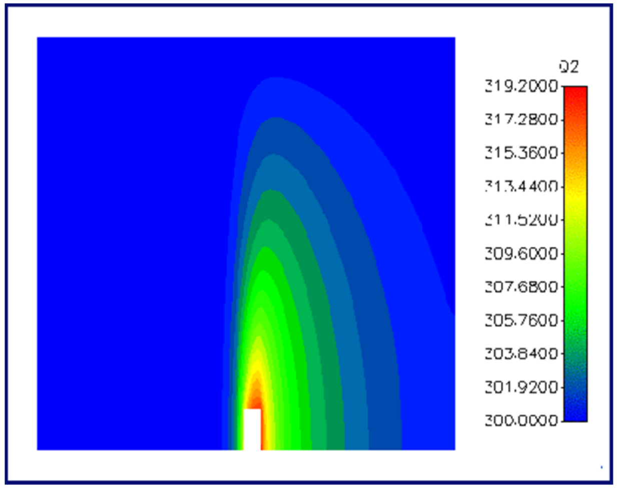

I_V small

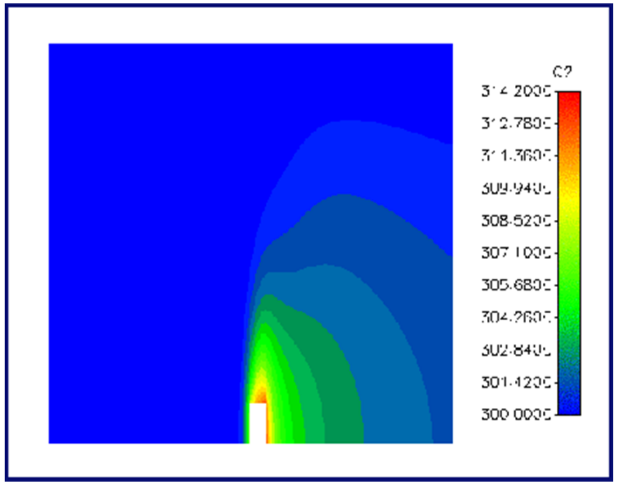

I_V large

- 1 heater
- 2 temperature sensors
  - T_1: temperature *before* heating
  - T_2: temperature *after* heating
- Temperature distribution dependent on flow profile or rate I_V
- Operating modes
  - Constant heat power P
  - Constant temperature of heater T_{heat}

7.2.4. Thermal Anemometer

Macro

- Thermal loss (thermal anemometer)
  - Heated membrane in contact with flow
  - Modus 1: constant temperature *T*
  - Modus 2: constant heat power *P*
  - Measurement of flow velocity v_{surf} above membrane
  - Calibration required

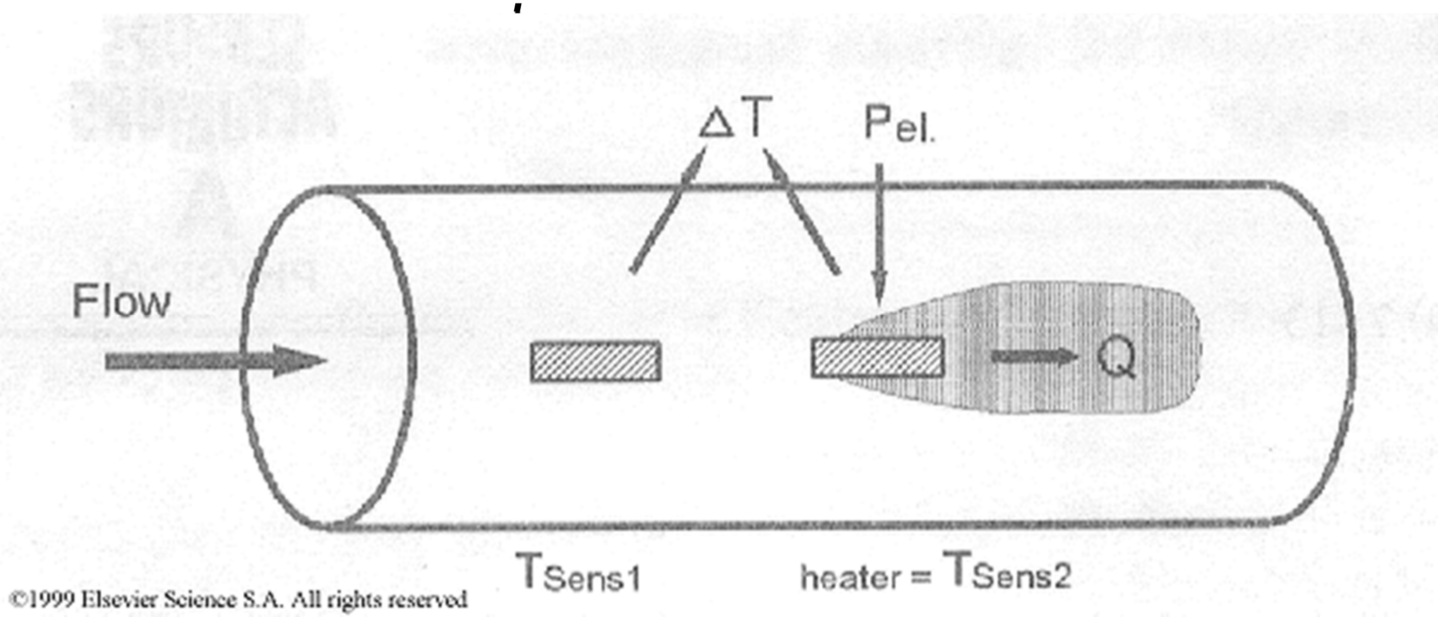

7.2.4. Calorimeter

Macro

- Principle of thermal transfer
- Heating of fluid
- Measurement of temperature difference ΔT
- Heat power P **directly related** to mass flow I_V

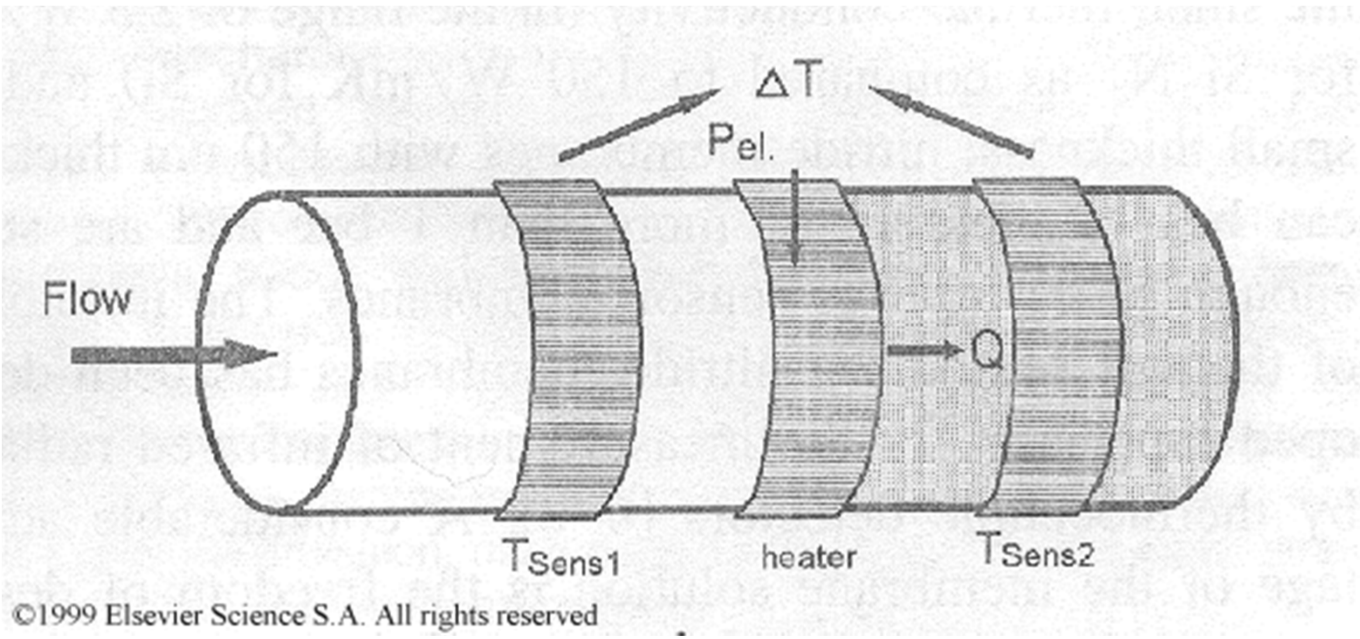

7.2.4. Principle of Micro Thermal Transfers

- Measurement of **change in *T*** like macroscopic thermal transfer
- Very **small** heaters and thermometer (few µm)
  - Low measurement-induced pressure drop
- Small **distances** (some 100 µm)
- Heat transfer limited to **fluid boundary layer**
  - Highly sensitive measurement
  - Small thermal masses / heat power involved

Micro

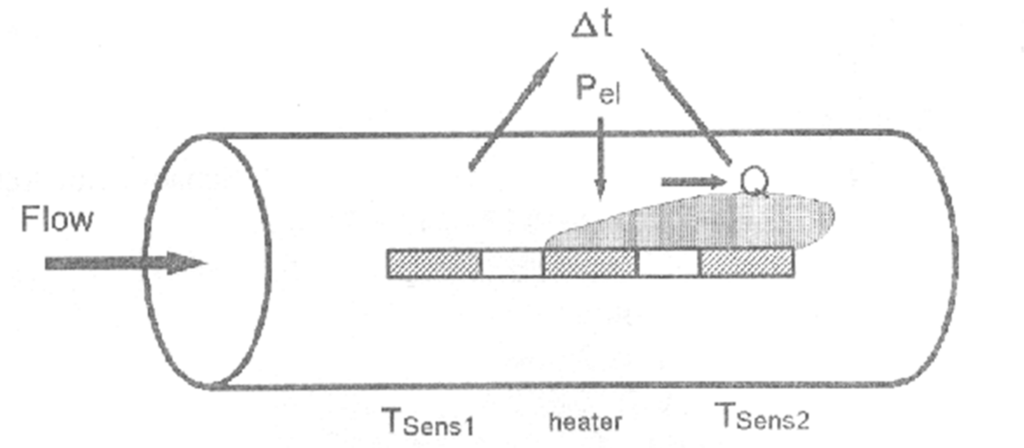

7.2.4. Thermal Time-of-Flight

- Low thermal masses allow **short heat pulses** (some ms)
  - ➢ Localized thermal signal
- Small distances translate into **short time intervals** (some ms)
  - ➢ Suppression of diffusive broadening
- Limitation of heat transfer to **boundary layer**
  - ➢ Distortion of temperature profile by flow profile

Micro

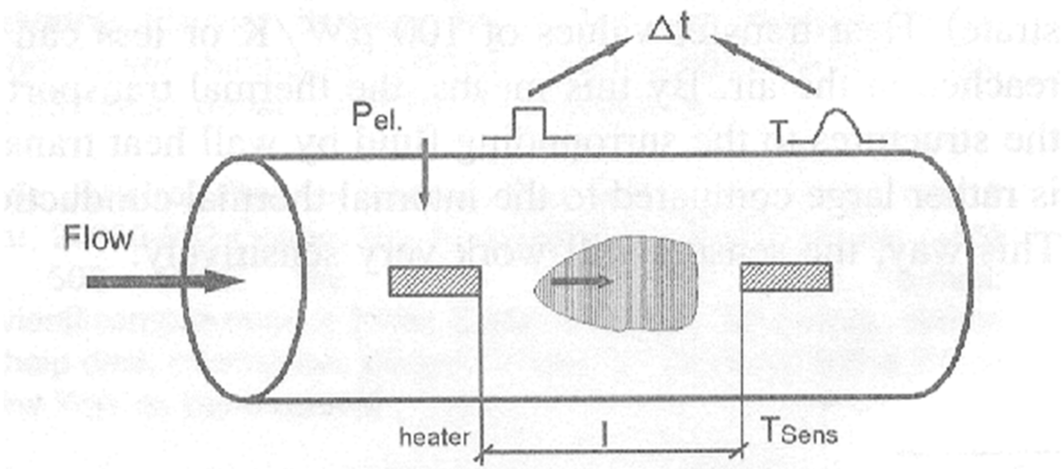

7.2.4. Thermal Flow Sensor for Liquids

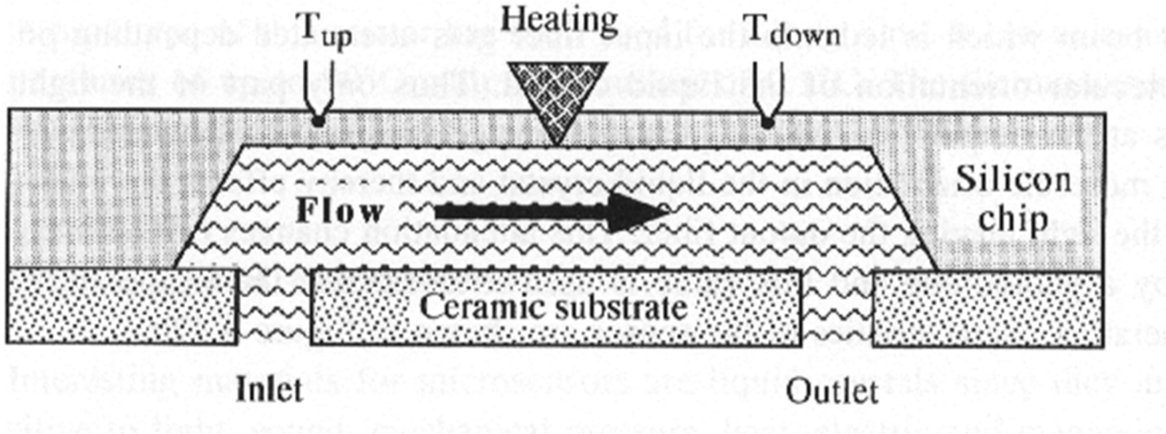

- Inlet and outlet in ceramic substrate
- Flow channel, central heater and *T*-sensor in Si-chip
- 1. Operating mode
  - 5 Hz signal of heater
  - Time delay of T_{down}
- 2. Operating mode
  - Constant heat power *P*
  - Measurement of difference $T_{up} – T_{down}$
  - Sensitivity 0.05 – 0.2 ml / min
- Drawback: possible change in liquid properties induced by heating

7.2.4. Thermal Flow Sensor for Gases

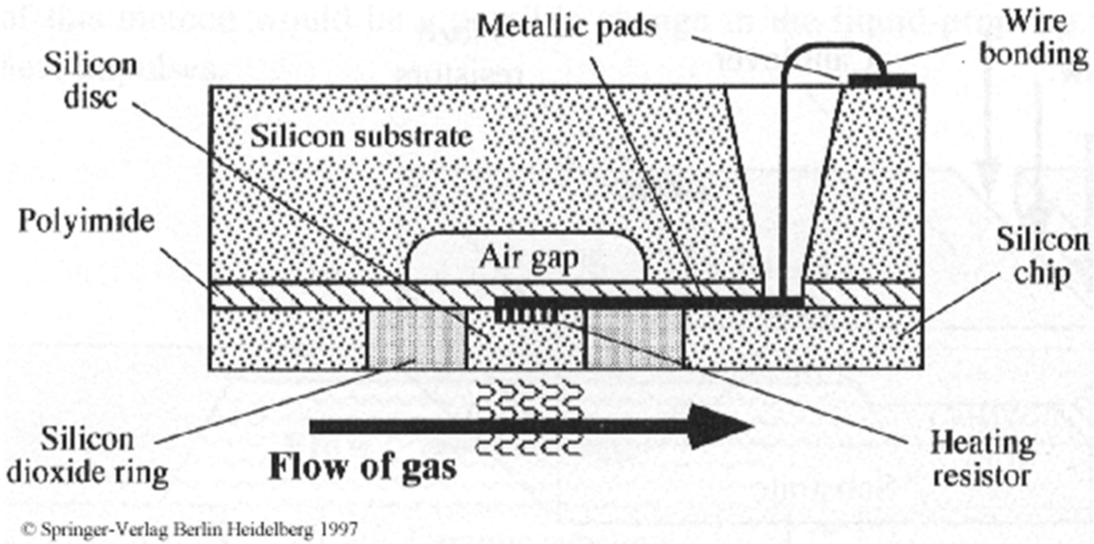

- Round Si disk with integrated heat resistor
- SiO_2-ring for insulation of heater from (cold) *T*-sensors
- Cover of chip by 3 µm polyimide film
- Dimensions: 5 x 5 mm^2
- Heating of gas above heated Si
- Two CMOS-diodes (not shown) measure *T*-difference
- Sensitivity: 10 cm / s, flow rates up to 2.5 m / s

7.2.4. Electro-Caloric Sensor: Setup and Working Principle

- Forced heat transfer
  - From heater
  - Onto passing fluids with given thermal conductivity
- Heat loss dependent on
  - Flow velocity
  - Flow rate (cross section of channel)
- Measured signal
  - *T*-difference

Quelle: Gerlach, Dötzel „Grundlagen der Mikrosystemtechnik“, Carl Hanser Verlag München (1997)

7.2.4. Transduction

- Thermo-resistive
  - Si-resistors as heaters and sensors
- Universal usability
  - *T*-measurement
  - *T*-difference
  - Heat power *P*
- Manufacturing well-compatible with microtechnology
- Low costs for mass fabricated sensors

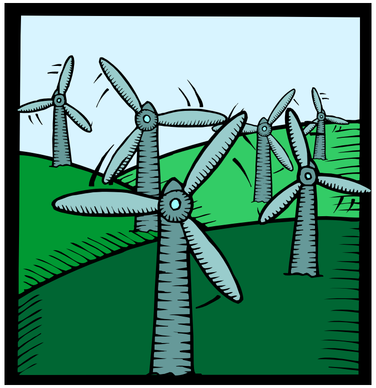

7.2.4. Operating Modes

- Constant heat power

$$P = const.$$

- Constant temperature of heater
  - ➢ Temperature difference between heater and fluid

$$\vartheta_0 = \vartheta_H - \vartheta_{Fl}$$

- Temperature difference between measurement points

$$\Delta\vartheta = \vartheta_2 - \vartheta_1$$

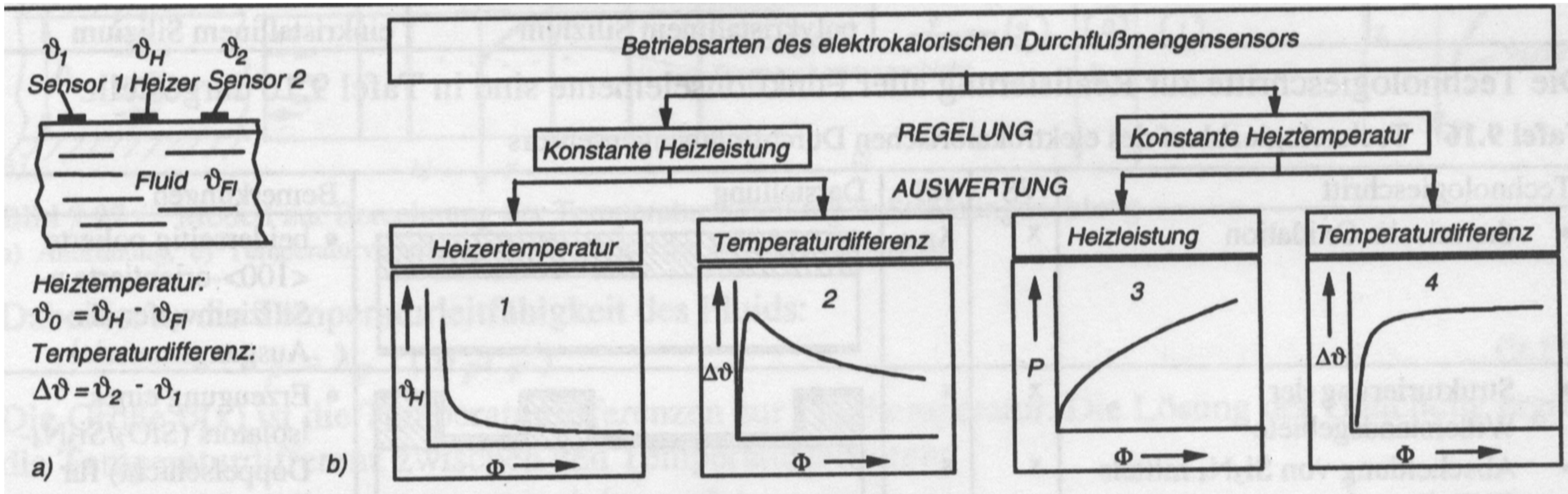

7.2.4. Chip Integration - Example

- Heaters and sensors on thin membrane
  - No direct contact to medium
- Resistive sensors
  - Diffusion-doped, monocrystalline <100>-Si
  - Positive temperature coefficient
- Resistive heaters
  - Polycrystalline Si
  - Negative temperature coefficient
- Resistive sensors geometrically small compared to heaters
  - Nearly point-like measurement of temperature

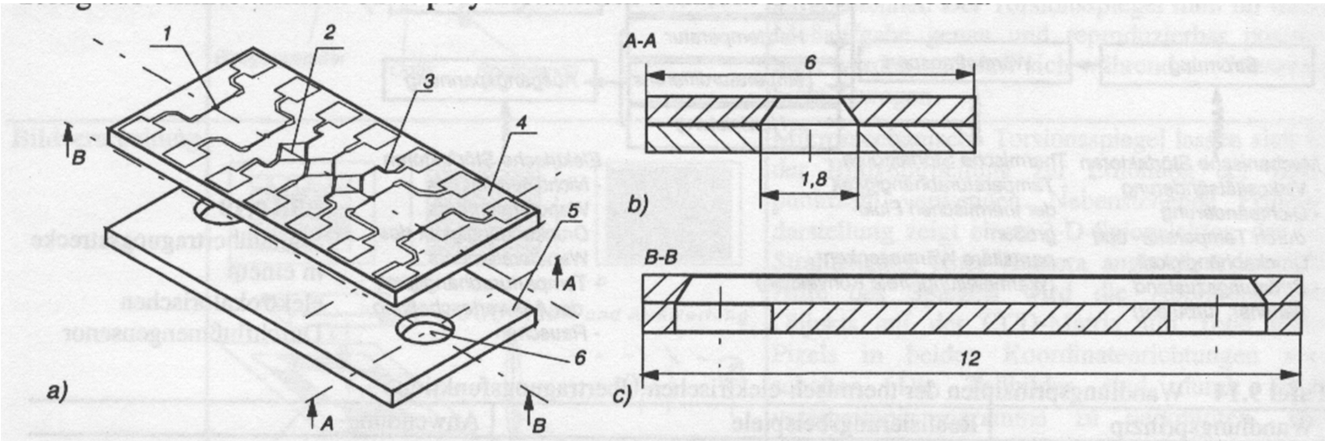

Bild 9.21 **Aufbau des elektrokalorischen Durchflußmengensensors aus Silizium**
a) Explosivdarstellung; b) Querschnitt; c) Längsschnitt; *1* einkristalliner Siliziumwiderstand; *2* polykristalliner Siliziumwiderstand; *3* Aluminiumleitbahn; *4* Siliziumchip; *5* Glasscheibe; *6* Ein-und Auslaßlöcher

7.2.4. Analytical Model for *T*-Distribution I

- Conservation of thermal energy

$$\left(\frac{1}{2}+\frac{\lambda_{\mathrm{Si}} d_{\mathrm{M}}}{\lambda_{\mathrm{F}}\delta}\right)\frac{\partial^2}{\partial x^2}\vartheta(x)-\frac{v}{2a_{\mathrm{F}}}\frac{\partial}{\partial x}\vartheta(x)-\frac{1}{\delta^2}\vartheta(x)=0$$

- Temperature difference to fluid $\vartheta(x)$
- Thermal conductivity of fluid $a_{\mathrm{F}}=\lambda_{\mathrm{F}}/\rho_{\mathrm{F}}c_{\mathrm{F}}$
- Parabolic flow profile (PDF)

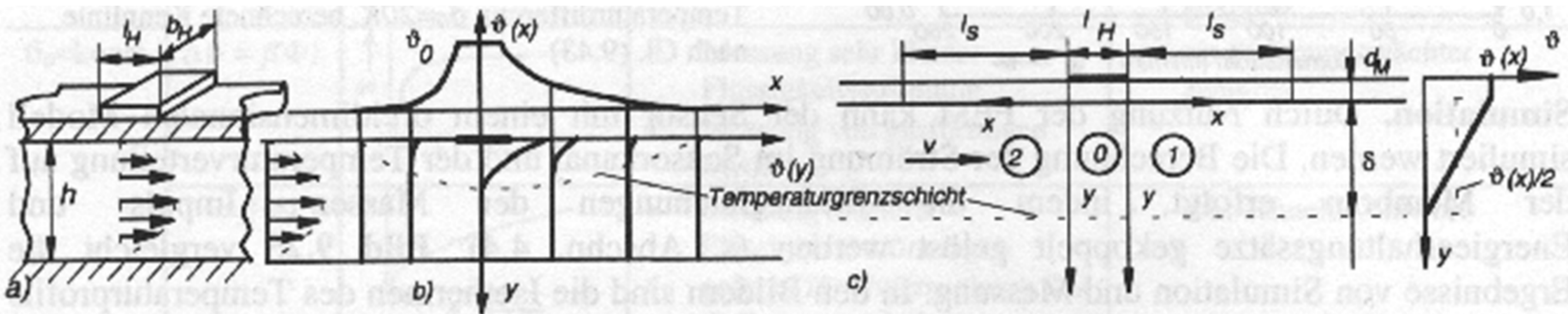

Bild 9.22 Modell zur Berechnung der Temperaturverteilung in Strömungsrichtung
a) Anordnung; b) Temperaturverteilung; c) Geometrie des Berechnungsmodells

7.2.4. Analytical Model for *T*-Distribution II

- Temperature difference between temperature sensors

$$\Delta\vartheta(l_S,\delta,v)=\vartheta_0\left(e^{k_2 l_S}-e^{-k_1 l_S}\right)$$

$$\text{mit}\quad k_{1,2}=\left(v\pm\sqrt{v^2+16a_F{}^2\kappa/\delta^2}\right)/4a_F\kappa\quad\text{und}\quad\kappa=\frac{1}{2}+\frac{\lambda_{Si}d_M}{\lambda_F\delta}$$

- Width of distribution $1/k_{1,2}$
- Factor κ: impact of Si-membrane on thermal transfer
- Temperature of resistive heater from heat power *P*

$$\vartheta_0=\boxed{P}/\left\{\lambda_F b_H\left[l_H/\delta+\sqrt{\boxed{v^2}\delta^2/4a_F{}^2+4\kappa}\right]\right\}$$

7.2.4. Analytical Model for *T*-Distribution III

- Characteristic curve of ***T*-difference** at **constant heat power *P***
  - Water, thickness of boundary layer equals height of channel $\delta = h = 500\ \mu\text{m}$

$$P = 0{,}25\,W, \quad b = 300\ \mu\text{m}, \quad l_H = 900\ \mu\text{m}, \quad l_S = 200\ \mu\text{m}$$

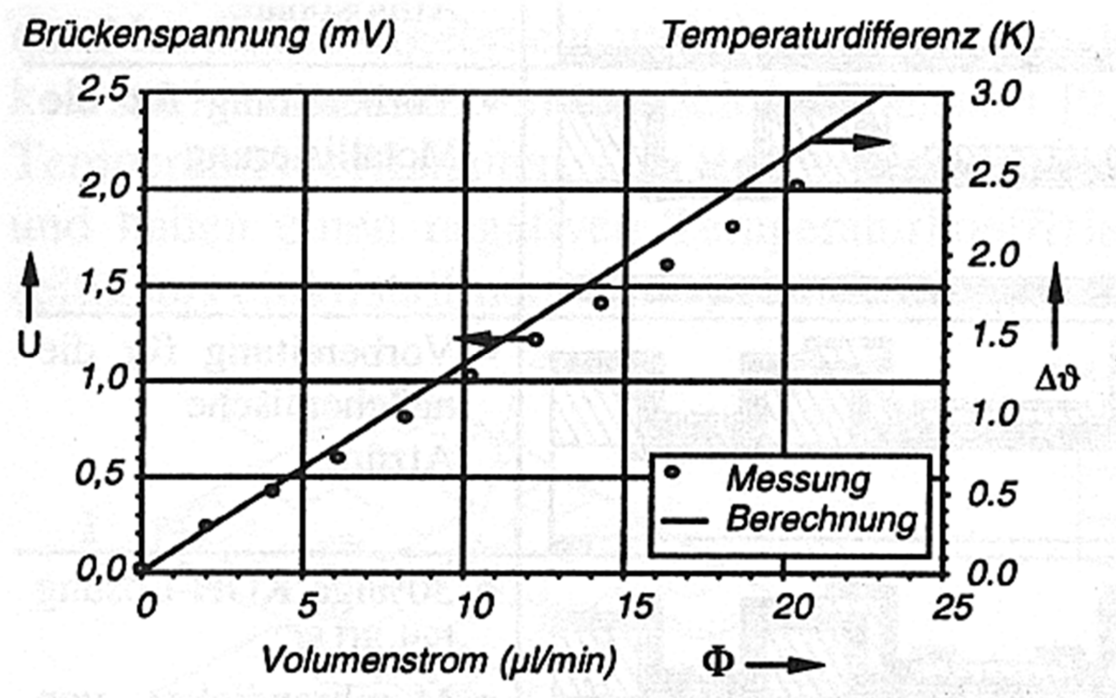

7.2.4. Analytical Model for Heat Power

- Characteristic curve of **heat power** at **constant heater temperature**
- Parameters

$$b_{\mathrm{H}} = 300\ \mu\mathrm{m}, \quad l_{\mathrm{H}} = 900\ \mu\mathrm{m}, \quad d_{\mathrm{M}} = 15\ \mu\mathrm{m}, \quad \vartheta_0 = 20\ \mathrm{K}$$

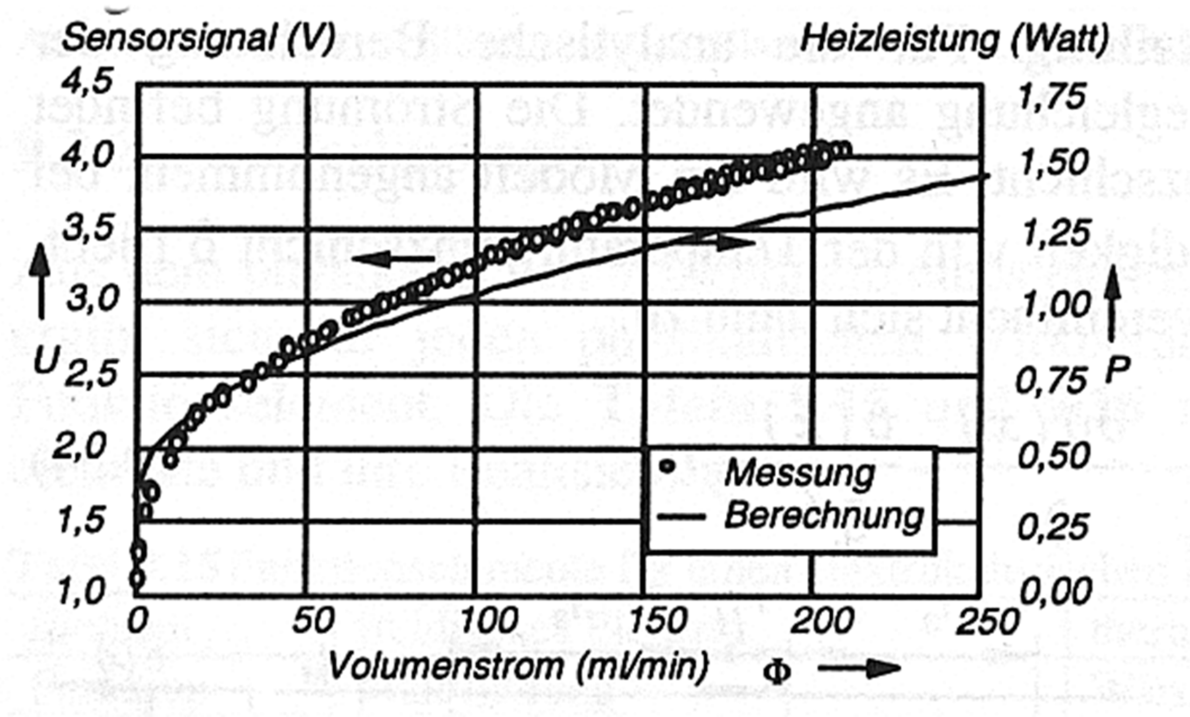

7.2.4. FEM-Simulation of *T*-Distribution

- 3-dimensional model
- Numerical solution of coupled equation
  - Mass
  - Momentum
  - Energy

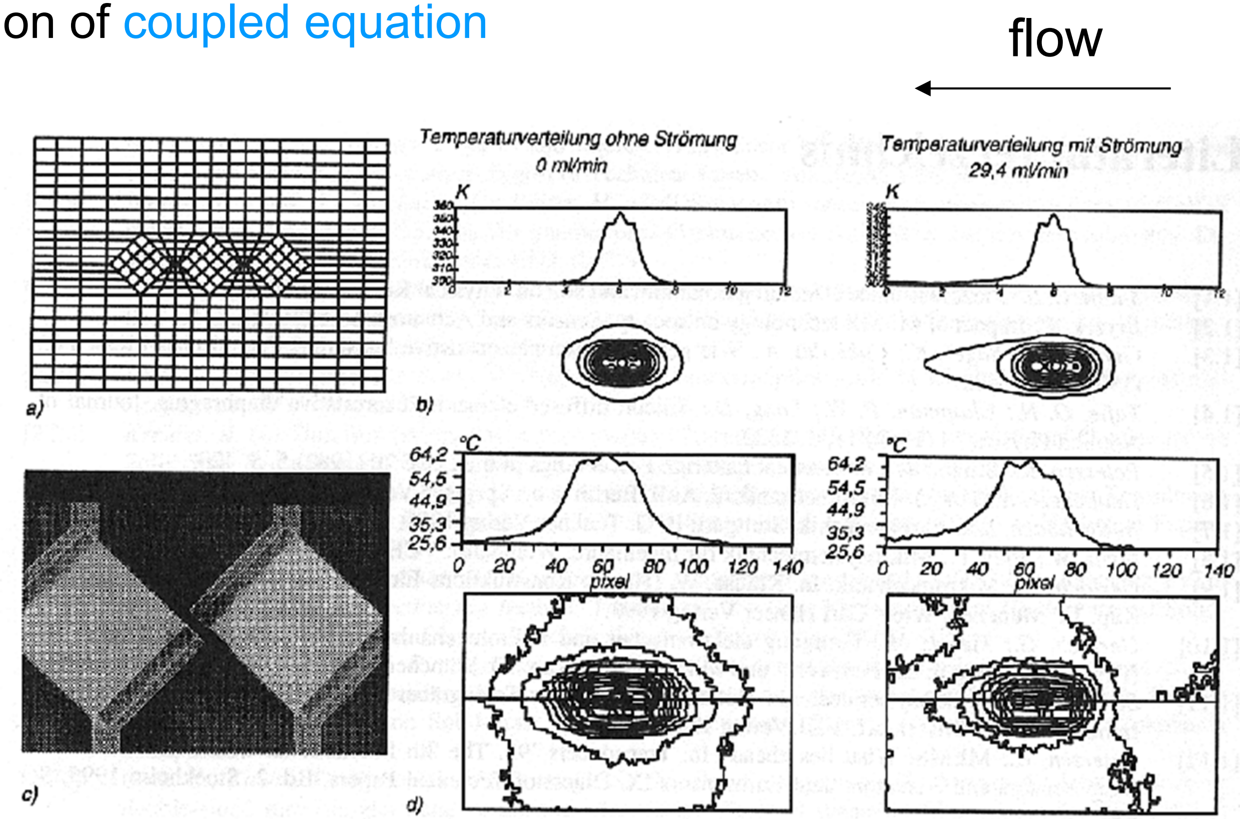

Bild 9.25 Temperaturverteilung auf dem Sensorchip
a) Modell; b) Simulation; c) Heizerstruktur; d) Thermografie

7.2.4. Development of *T*-Signal in Flow Profile

- Numerical simulation
- Pulse width: 2 ms
- Power: 70 mW
- Flow velocity: 90 mm / s
- Observation after: 2 ms (left) und 20 ms (right)

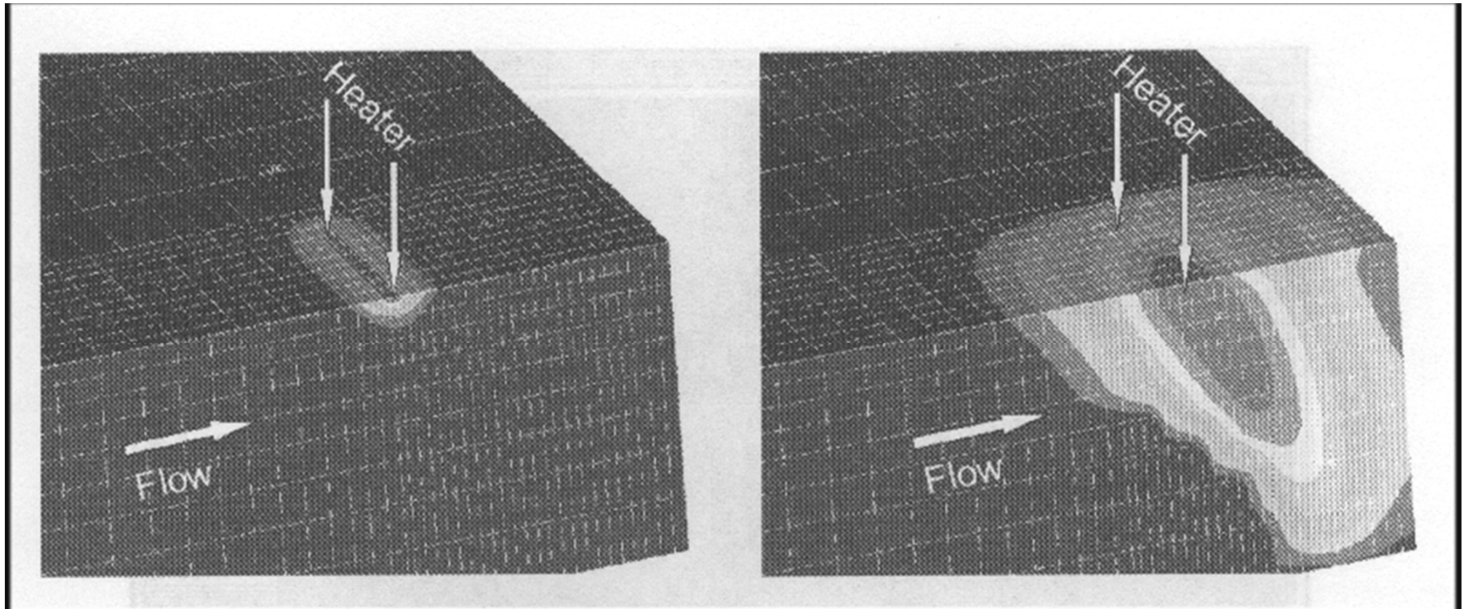

7.2.4. Thermal Flow Sensor: Setup

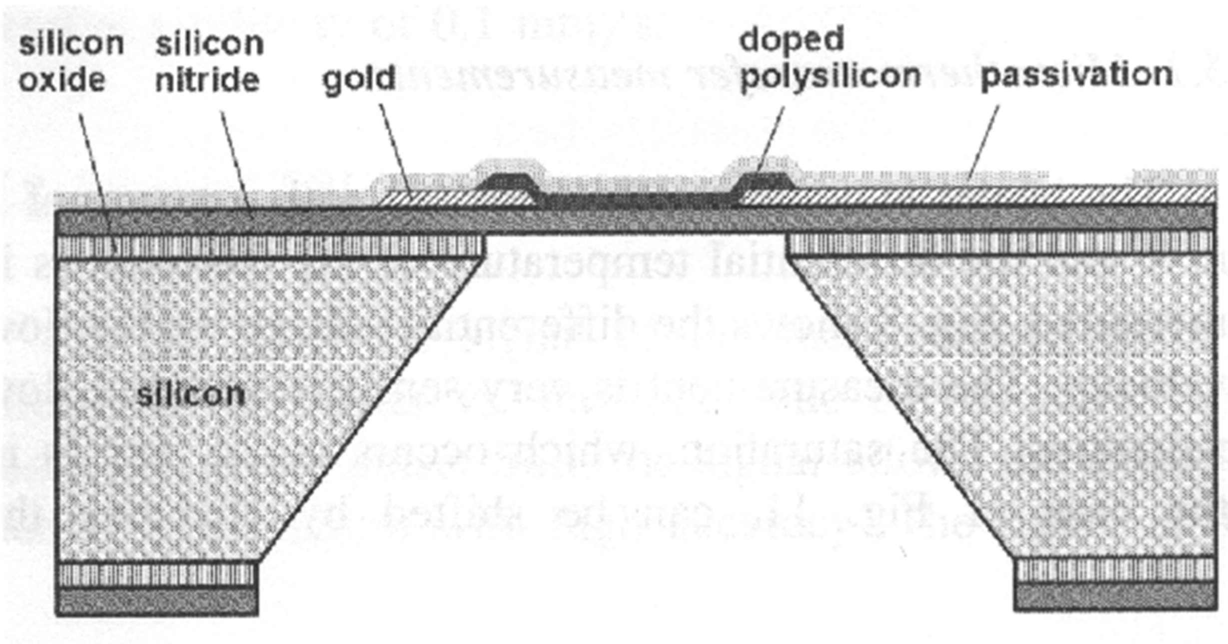

7.2.4. Prozess Technology

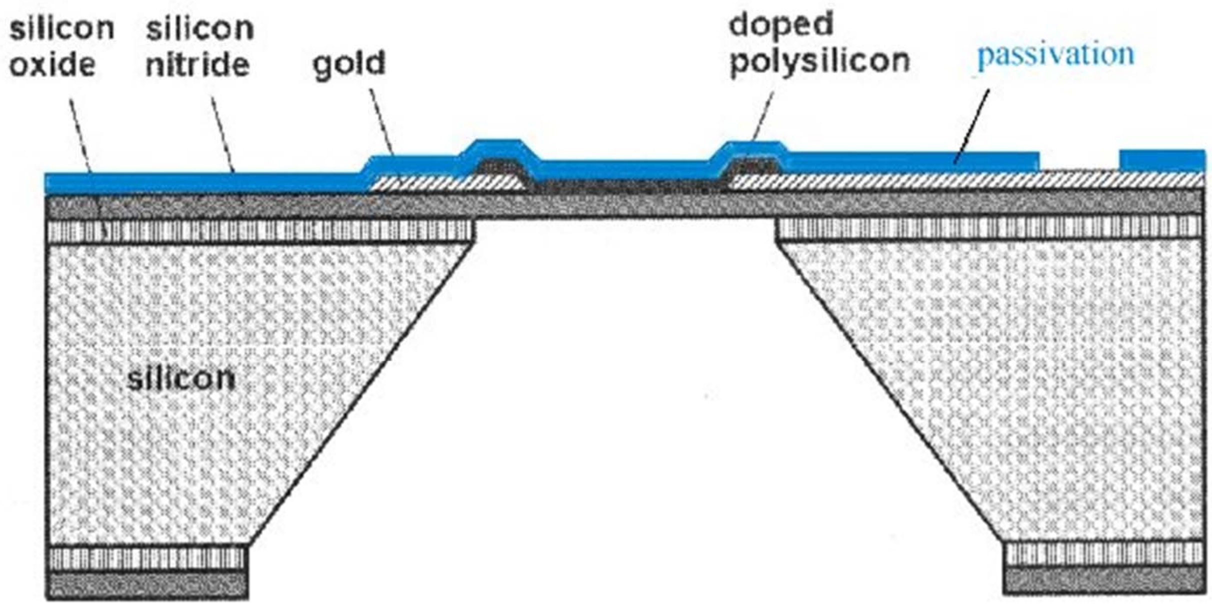

7.2.4. Thermal Anemometer

- Membrane surface: 600 μm^2
- 20 thermopiles in series
- Heaters in center
  - Width: 5 and 15 µm
  - Distance to hot thermopile: 10, 75 and 150 µm
- Different designs optimized for particular dynamic range

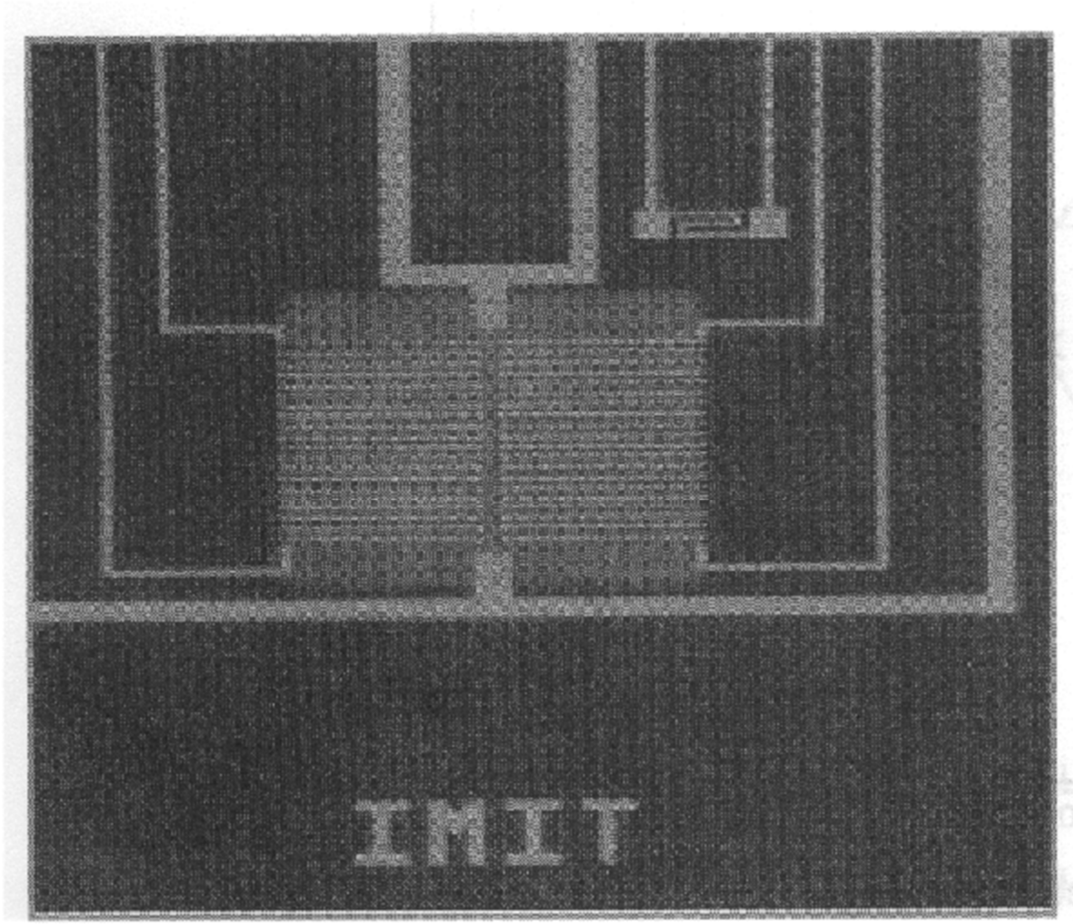

7.2.4. Thermal TOF Anemometer

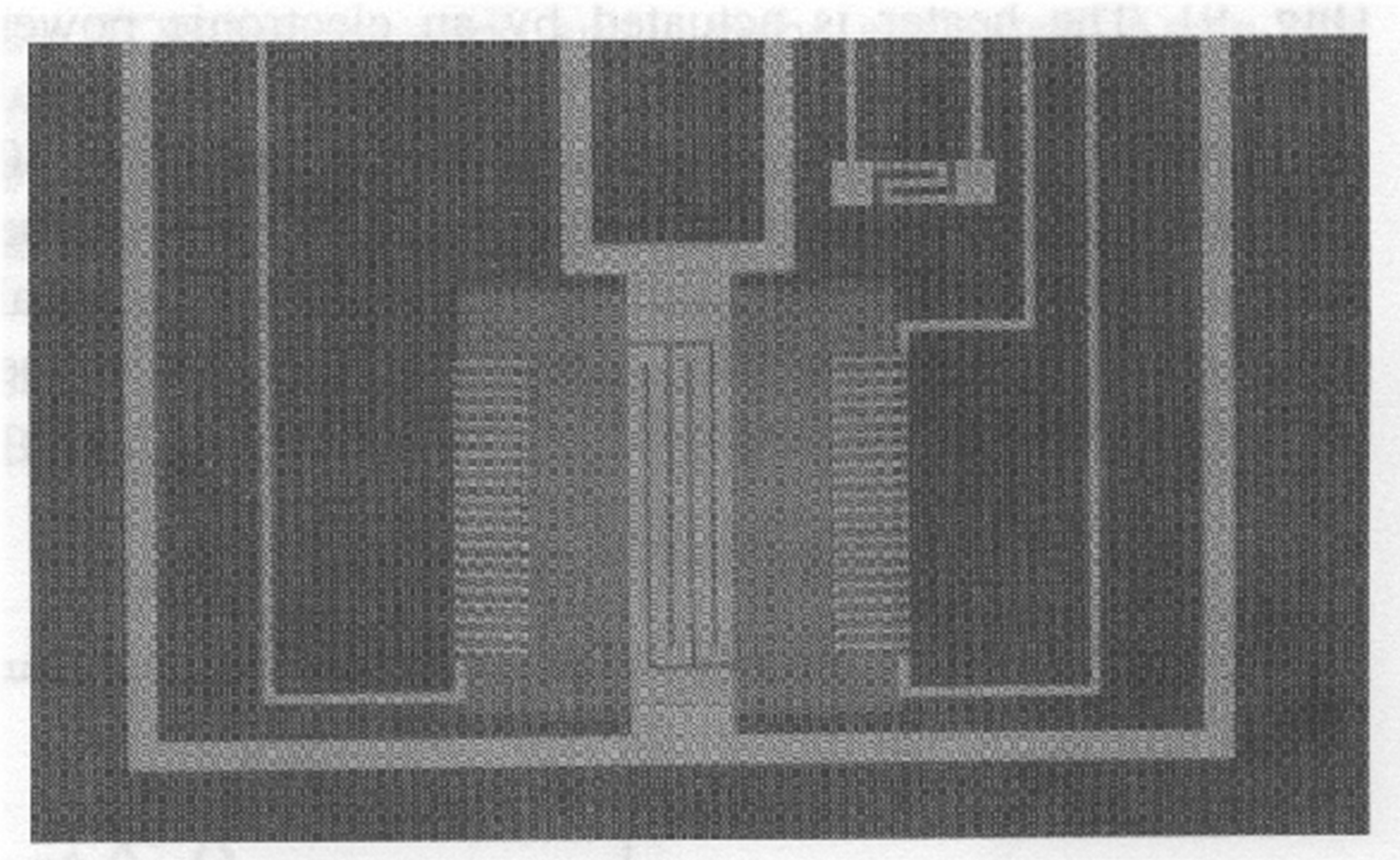

7.2.4. Measurements

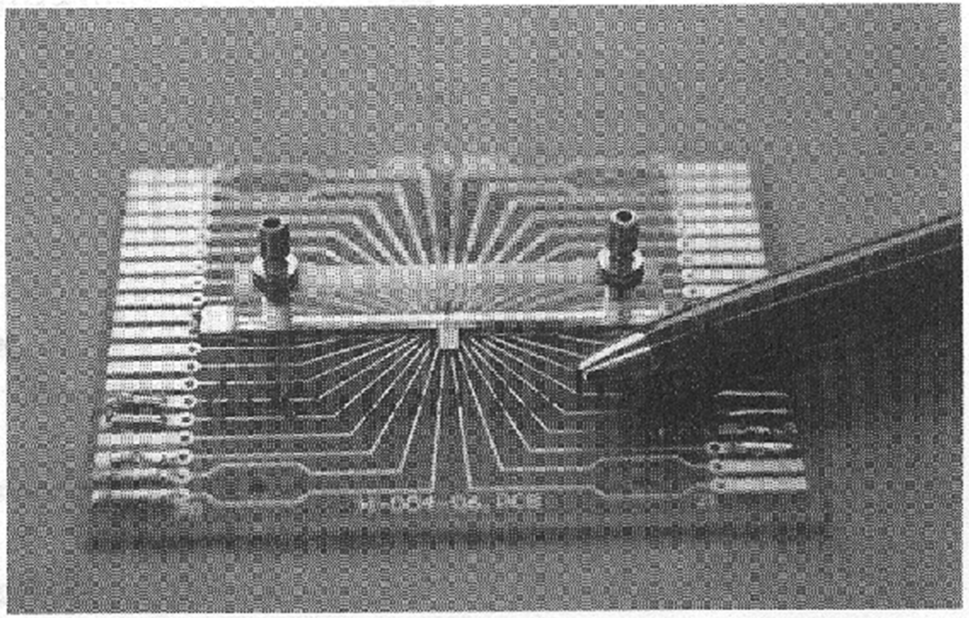

- Flow channel (cross section: 0.4 mm x 0.6 mm) mounted on sensor
- Constant heat power *P*
- **Signal processing**
  - Electric heat power: 50 mW
  - Thermal signal generated by a few nW available at location of sensor
  - Electric signal: some pW
  - Preamplifier and filter required

7.2.4. Evolution of *T*-Distribution

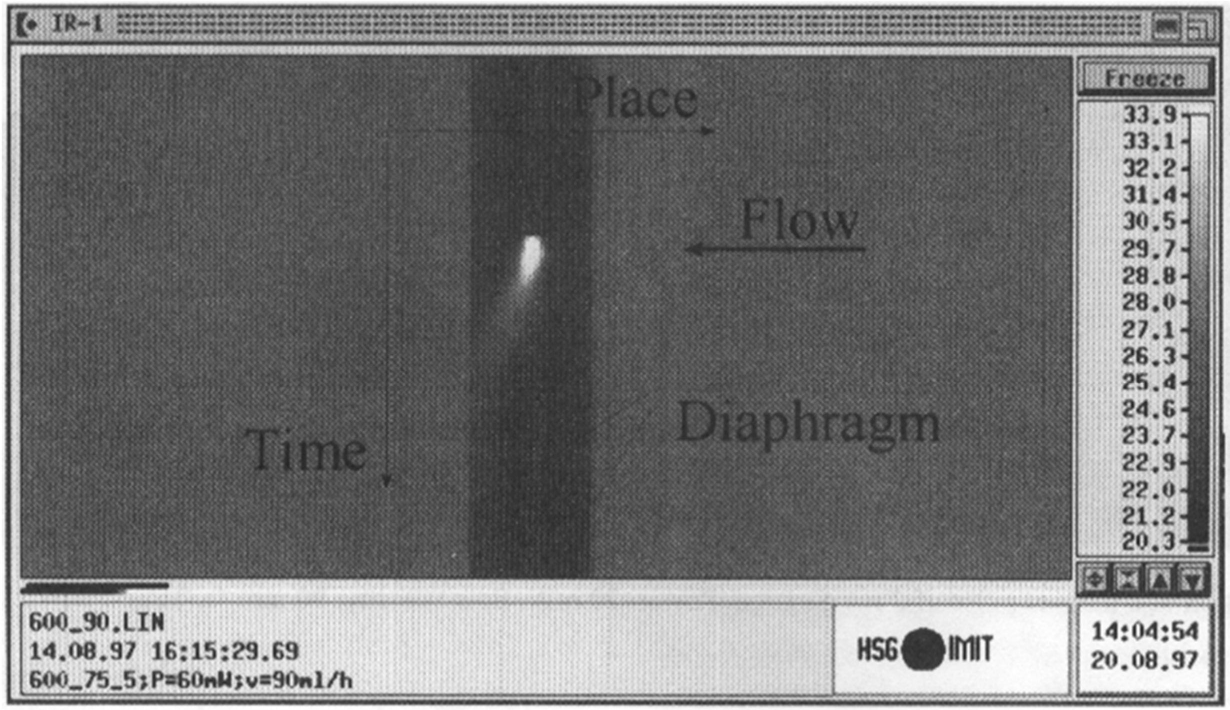

- IR camera
- Scan-line mode
- Vertical: time axis (origin on top)
- Horizontal: subsequent line-scans across sensor

7.2.4. Calibration of Thermal Anemometer

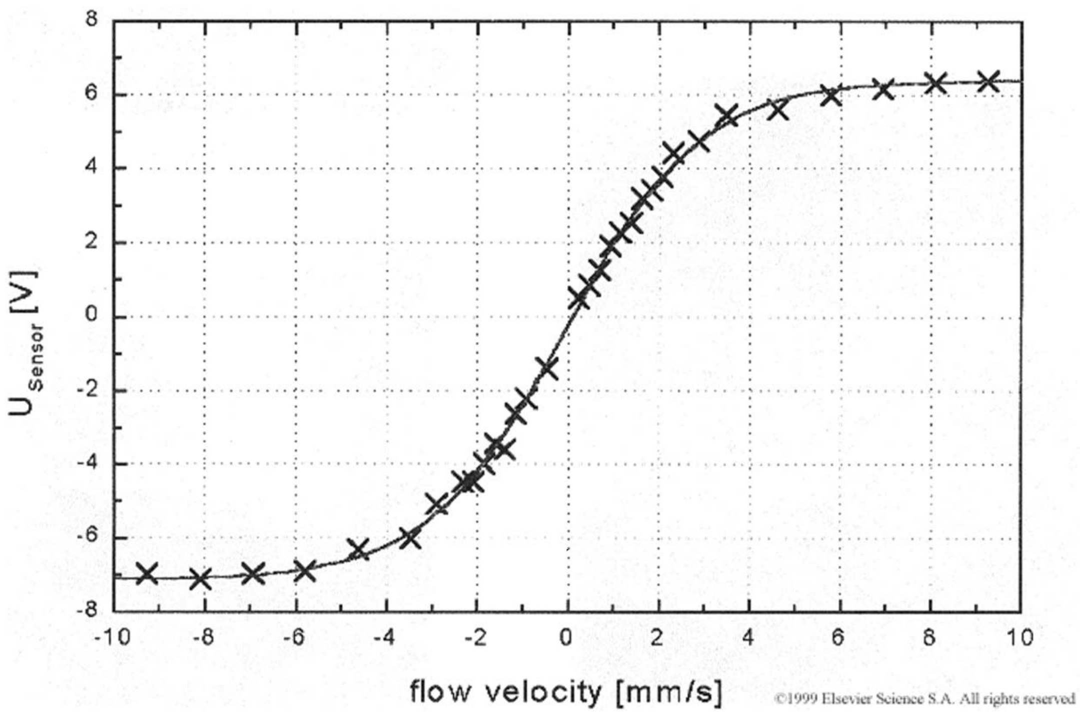

- Thermo-voltage U_{sensor} (amplified) against flow velocity *v*
- High sensitivity (slope) at low *v*
- Resolution: 0.1 mm / s
- Saturation at *v* = 2.5 mm / s
- Saturation value controllable by geometry
- Bidirectional sensor

Microprocessor

7.2.4. Time-of-Flight Measurement

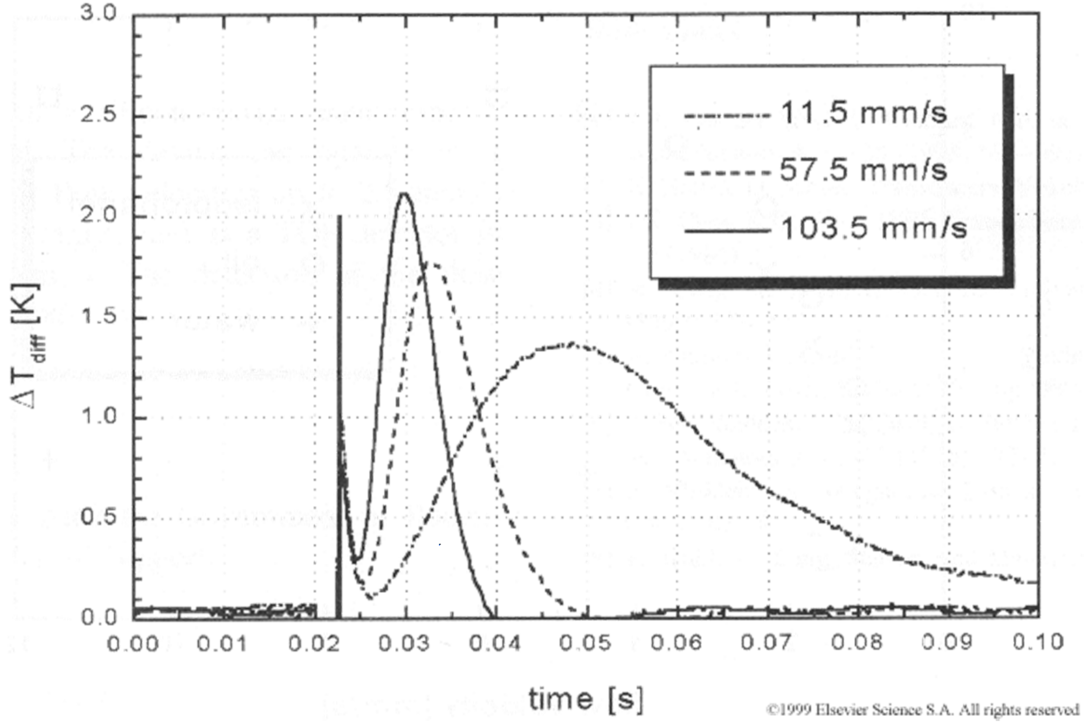

- Temperature difference ΔT_{diff} against flight time t
- Narrow initial pulse: **crosstalk** of heat pulse
- Increasing **broadening** of measured pulse with decreasing v
- Good **separation** between two pulses
- Well defined **maximum** of pulse

Microprocessor

7.2.4. Integration of Both Principles

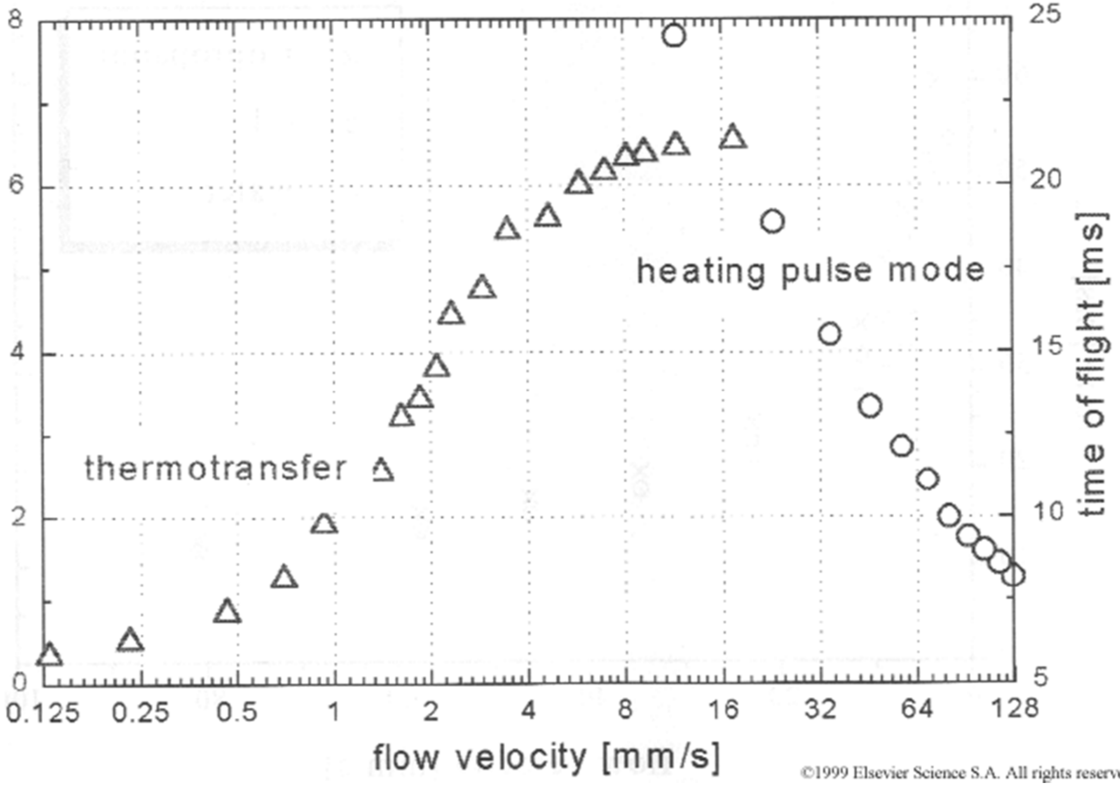

- TOF at medium flow rates of about v = 140 mm / s
- Thermal transfer at low velocities up to v = 0.1 mm / s
- Combination of principles in same device by smart design
  - Wide measurement range in single sensor

7.2.4. Micro-Thermotransfer with Different Fluids

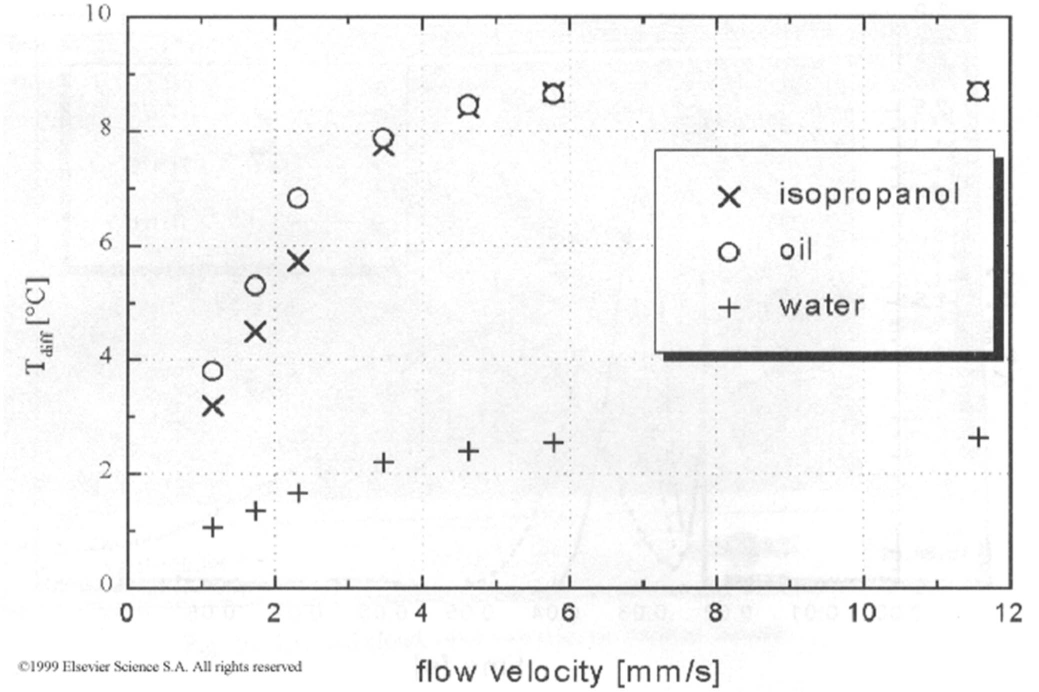

- Measurements with **water**, **oil** and **isopropanole**
- Thermal transfer in boundary layer
- Thickness of boundary layers depends on
  - Thermal conductivity
  - Viscosity
- Method of microthermotransfer to be calibrated for each liquid!

7.2.4. Micro-Thermotransfer with Different Fluids

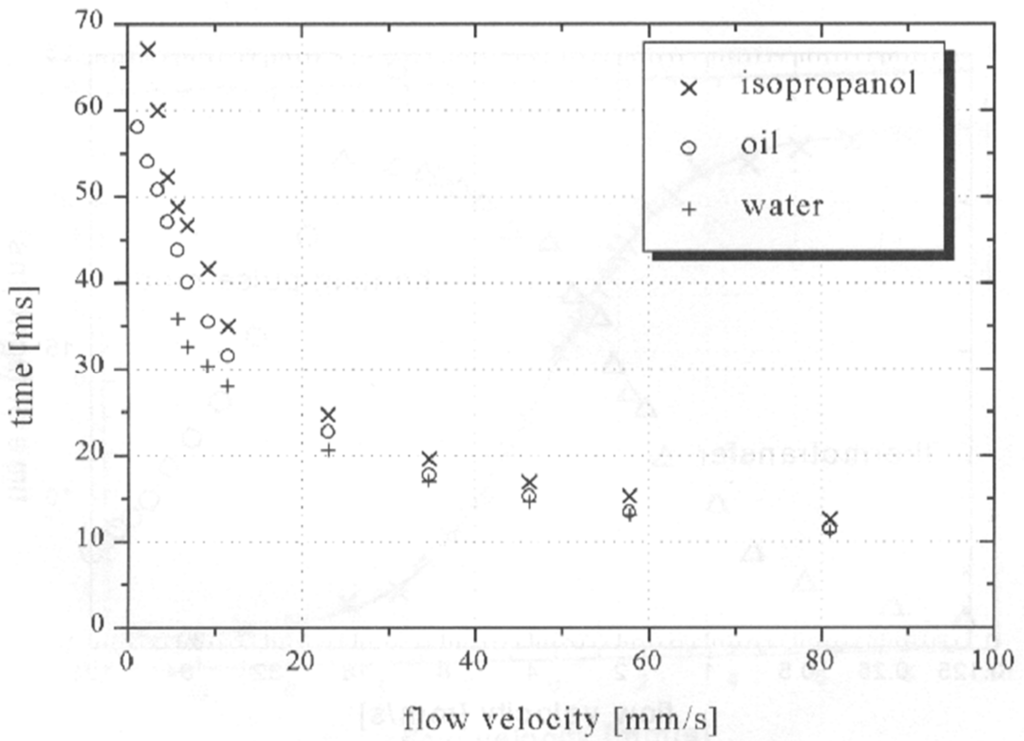

- Time signal, propagating with fluid
- Measurement principle widely independent from properties of fluid

7.2.4. Further Configurations

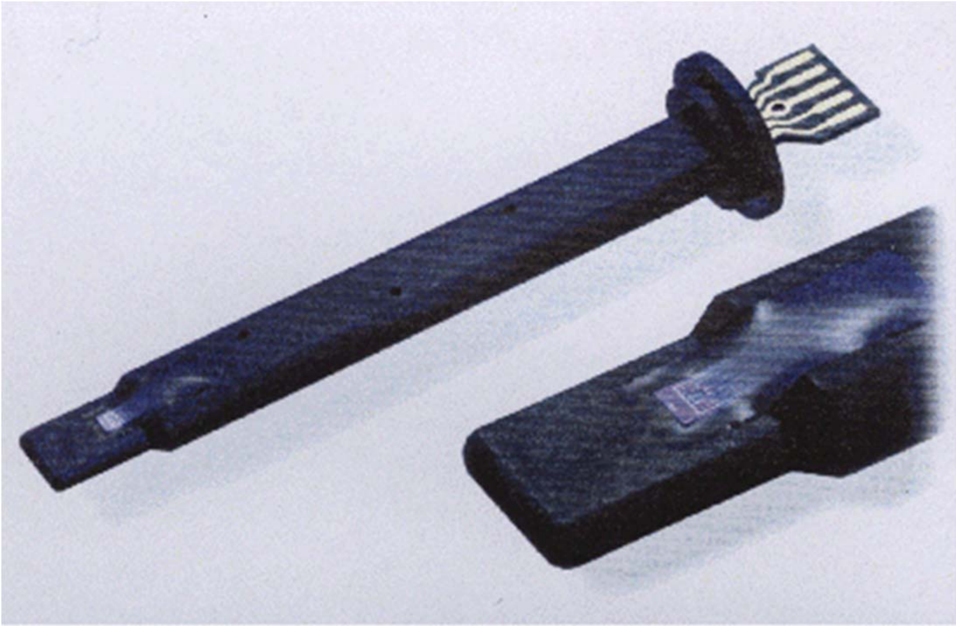

Air mass sensor for free currents

Length from flange to chip:
ca. 50 mm

Flow velocities:
0 – 100 m / s

7.2.4. Further Configurations

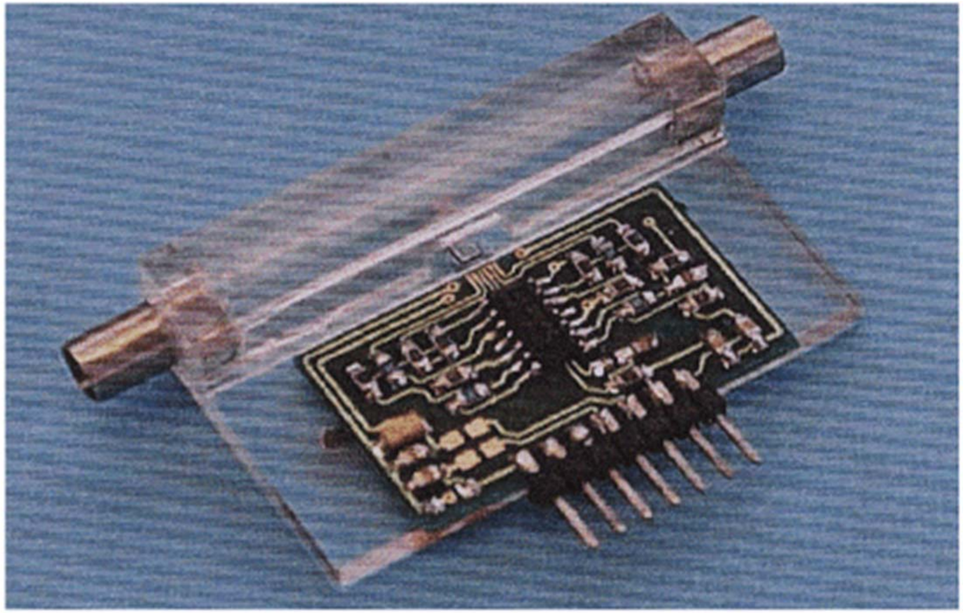

Volume flow rate sensor
in measurement channel

Diameter: D = 4 mm
D between
0.5 mm and 6 mm possible

Volume flow:
For water: 0 – 1 l / min
For gases: 0 – 100 l / min

7.2.4. Further Configurations

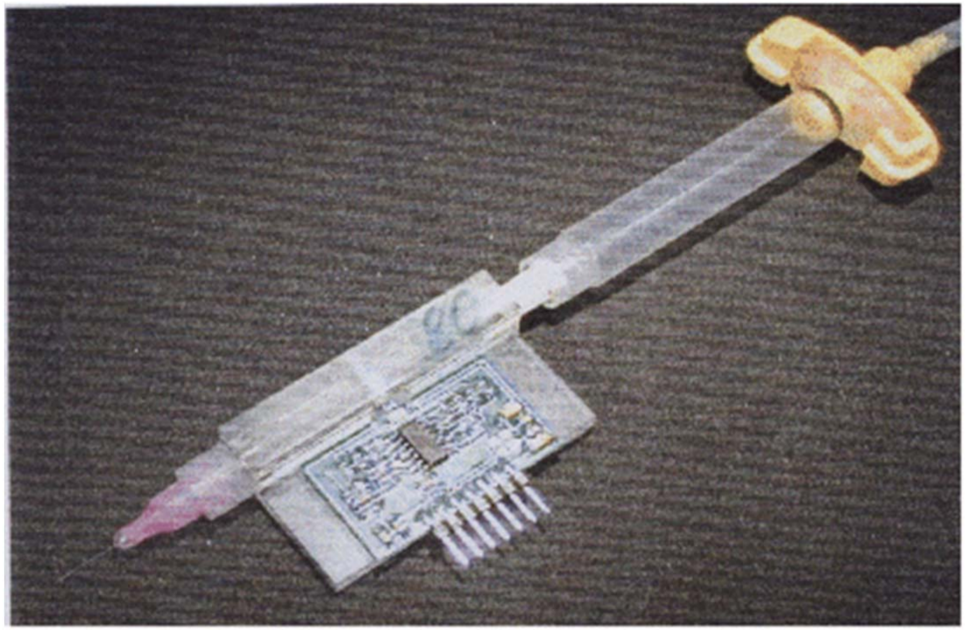

Special configuration for dosage tools

Minimum volume flow:
1 µl / min

Temporal resolution:
below 10 ms

⇒ Resolution for dosage: 0.2 nl

7.2. Flow Sensors

1. Physical Sensor Components
2. Drag-Force Flow Sensors
3. Differential Pressure Flow Sensors
4. Thermal Flow Sensors
5. EHD Mass Flow Sensors
6. Coriolis Mass Flow and Density Sensor
7. Meniscus Detection

7.2.5. EHD Mass Flow Sensors

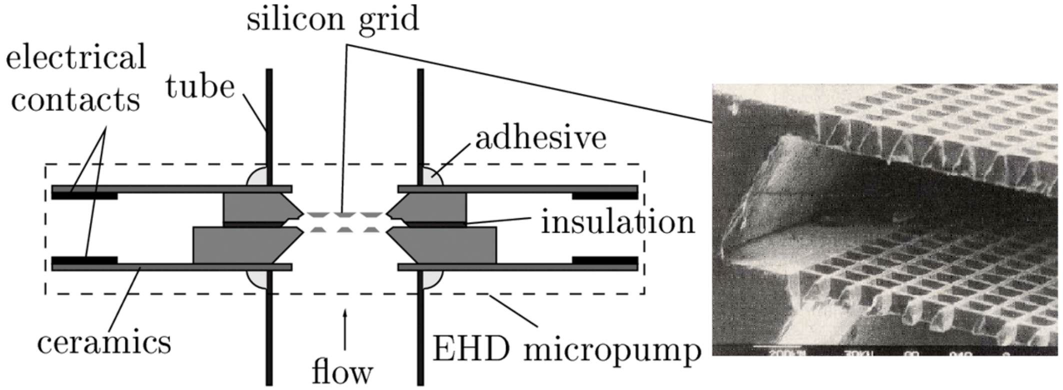

Fig. 6.27. Electrodynamic pump developed at FhG–IFT, Munich . Charge carriers in an insulating liquid are accelerated between the electrode grids

Electrohydrodynamic micro flow meter

- Analogy to EHD pumping
- Time of flight measurement of charge signal
- Charge pulse generated and picked up by two separate grids
- EHD principle confined to liquids exhibiting high electric resistivity
- Measurement induces EHD pumping
  - ➢ Possible interference with measurement
- Additional upstream electrode grid can eliminate this effect

7.2. Flow Sensors

1. Physical Sensor Components
2. Drag-Force Flow Sensors
3. Differential Pressure Flow Sensors
4. Thermal Flow Sensors
5. EHD Mass Flow Sensors
6. Coriolis Mass Flow and Density Sensor
7. Meniscus Detection

7.2.6. Resonant Fluid Density & Coriolis Mass Flow Sensor

- Tube system of silicon
- Oscillated in mechanical resonance
- Densitometer
  - Change in density of liquid flow inside tube
  - Change in resonance frequency of vibrating tube
- Coriolis mass flow sensor
  - Liquid flow in tube structure
  - Superimposed twisting of structure
  - Measured twisting due to Coriolis pseudo force proportional to liquid mass flow

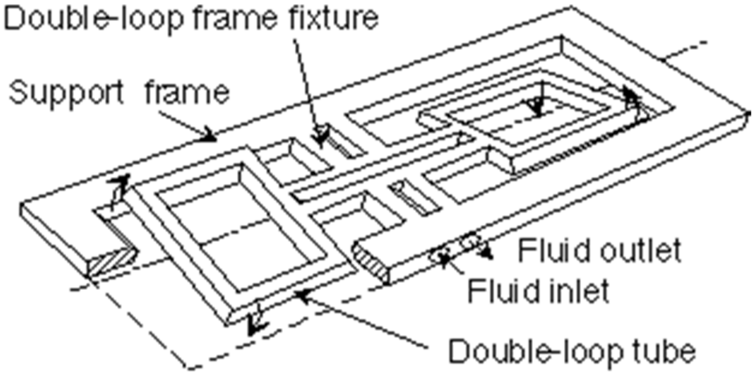

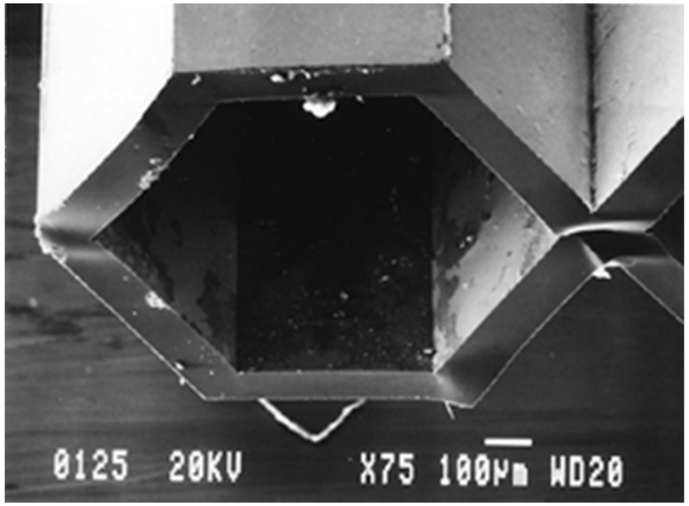

KTH Instrumentation Laboratory

7.2. Flow Sensors

1. Physical Sensor Components
2. Drag-Force Flow Sensors
3. Differential Pressure Flow Sensors
4. Thermal Flow Sensors
5. EHD Mass Flow Sensors
6. Coriolis Mass Flow and Density Sensor
7. Meniscus Detection

7.2.7. Meniscus Detection

- Transparent substrate
  - Precise, automated control of fluid volumes inside glass capillaries
- Linear CCD array
- Digital signal processor
- Real-time positional control with resolution of 50 µm

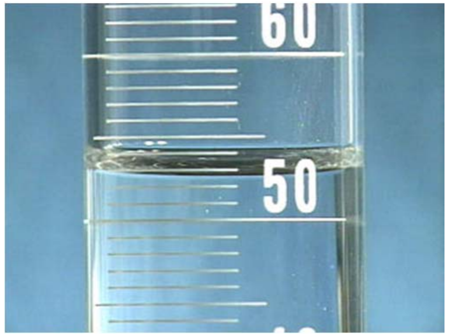

7.2. Flow Sensors: Summary

- Working principles of micro flow sensors
  - Optical / non-invasive (also flow field)
  - Mechanical
  - Differential pressure
  - Thermal
    - Anemometric
    - Calorimetric
    - Time-of-flight
- Examples for setup of performance of flow sensors
  - Electro-calorimetric sensor
    - Operating modes
    - Modelling of thermal transfer
  - Anemometer of HSG-IMIT
    - Calorimetric mode
    - Time-of-flight mode
  - Pressure sensor of HSG-IMIT
    - Differential pressure measurement in flow channel
  - Mechanical cantilever sensor
  - Coriolis-force sensor of KTH

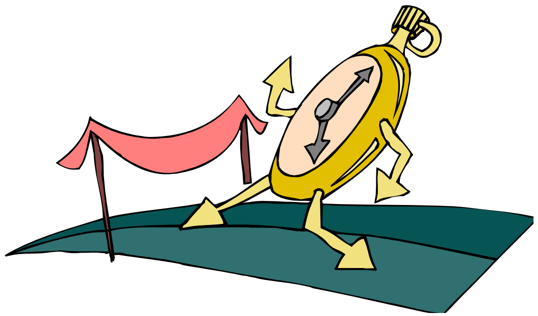

7. Sensors

1. Non-invasive sensing
2. Flow Sensors
3. **Chemical Sensors**

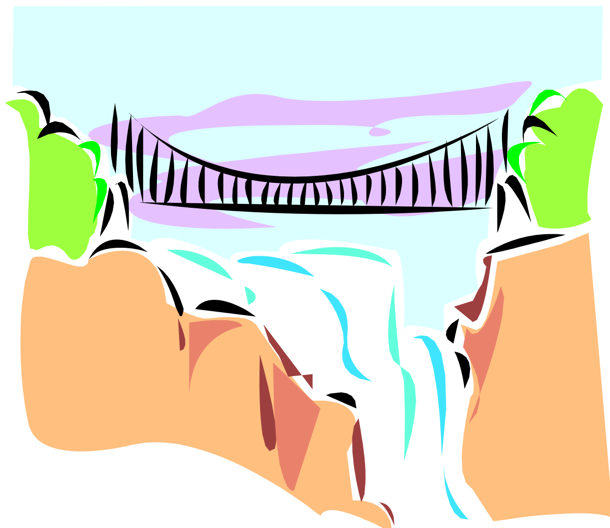

7.3. Chemical Sensors

Ideal Chemical Sensor

Signal generated by interaction of species of interest at interface between sensor and solution excluding all other species present

7.3. Chemical Sensors

1. Optical Detection
2. Electric Impedance Detection
3. Chemical Detection by Semiconductors
4. Biosensors

7.3.1. Optical / Radiative Detection

- Equipment
  - ➢ Stimulator for light emission, e.g.
    - Radiation source (laser, LED)
    - Chemical energy (chemiluminescence, …)
  - ➢ Detector
- Integrated measurement
  - ➢ Optical elements
    - Lenses
    - Beam guidance
  - ➢ Glass substrate plate
- Mearuement principles
  - ➢ Refractive index
  - ➢ **Absorption**
  - ➢ **Luminescence**
    - Fluorescence
    - Chemiluminescence
    - Bioluminescence
  - ➢ Optical activity
  - ➢ **Scattering**

7.3.1. Fluorescent Detection

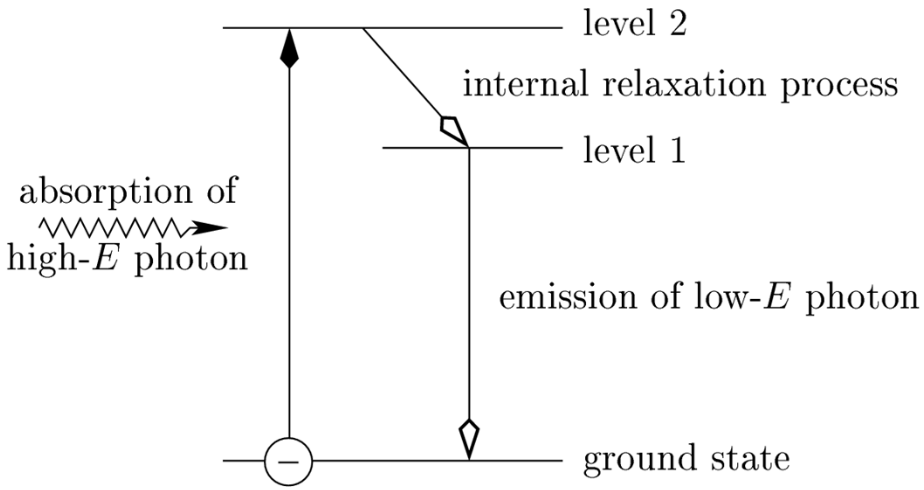

Fig. 2.31. Principle of laser-induced fluorescence. In a three-level atomic system, an electron is elevated by absorbing a high-energy photon from the coherent laser field to the upper level 2. Part of the energy is released by an internal process. The final relaxation step proceeds under emission of a low-energy photon which is used as the fluorescence signal

- Counting fluorescent bursts from individual, laser-excited molecules
- Laser excitation source
- Photo counter

7.3.1. Fluorescent Waveguide Sensor

- Waveguide coated by probe molecules
- Fluorescently labeled target molecules attach
  - Specific binding to probes
- Excitation beam coupled into waveguide by grating
- Modes in waveguide result in enhanced intensity of radiation field
- Evanescent field excites bound target molecules while intensity too low to initiate fluorescence of unbound molecules
- Fluorescent signal partially leaves waveguide via grating towards detector recording intensity
- Surface-sensitive detection, no washing required

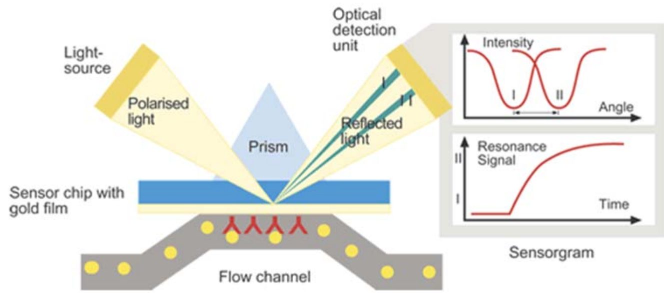

Biacore AB

7.3.1. Chemiluminescence

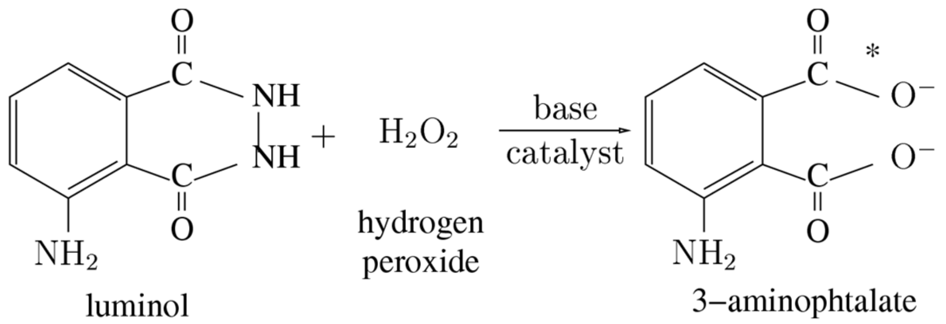

Fig. 2.32. Luminol is excited by an oxidation reaction with hydrogen peroxide. The excited 3-aminophtalate relaxes by the emission of light

- Mechanism
  - Low-temperature chemical reactions, chiefly oxidations, with „fuel“
  - Excited state product
  - Conversion of chemical into radiative energy (photons)
- Single photometric detector
- No excitation source
- Detection limit by factor of 10 to 100 smaller than luminescence

7.3.1. UV Absorption

- Optical absorption spectroscopy, in particular UV spectroscopy
  - ➢ Widely used in macroscopic analytical devices
    - Online detection method
  - ➢ Most materials used for microfabrication
    - Cut off wavelengths below 300 – 250 nm

- Microsystems
  - ➢ Optical spectroscopy feasible
  - ➢ Measurements in UV range not possible
    - UV transmitting quartz materials generally hard to integrate in microfabrication process

7.3.1. Thermal Lens Microscope

- *T*-dependence of refractive index *n*

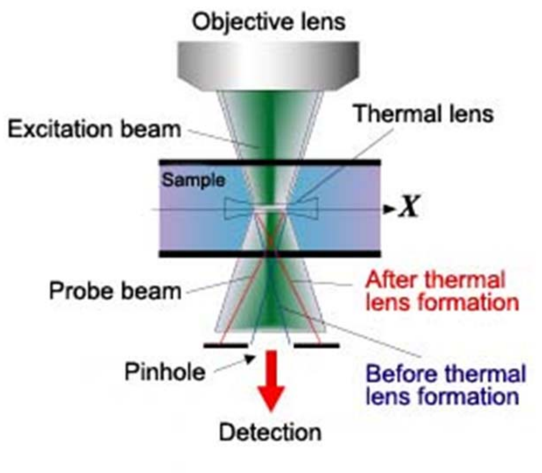

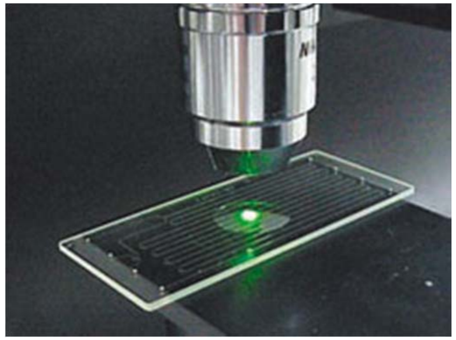

IMT Products

TLM measurement examples

Detection limit	Solute	Media
0.4 molecule	Porphyrine	Benzene
50 molecule	Dye molecule	Water
7 molecule	DNA	Poly-acrylamide gel
1 molecule	10-nm-sized Ag colloid	Water

7.3.1. Hyper-Rayleigh Scattering

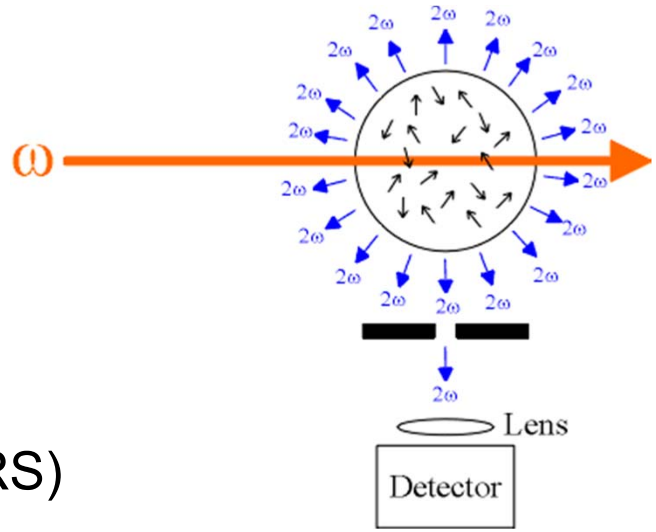

- Hollow capillary simultaneously
  - Fluid carrying medium
  - Leaky
    - *n*(fluid) usually smaller than *n*(substrate)
  - Optical waveguide
- Application in hyper Rayleigh scattering (HRS)
  - Measurement technique based on hyper-polarizability of optically nonlinear, organic molecules
  - Instantaneous fluctuations of otherwise homogeneous solution
  - Production of frequency-doubled light
  - Measurement of solute concentration
    - Prerequisite: known hyperpolarizabiliy of solvent

7.3. Chemical Sensors

1. Optical Detection
2. Electric Impedance Detection
3. Chemical Detection by Semiconductors
4. Biosensors

7.3. Chemical Sensors

7.3.3. Chemical Detection by Semiconductors

- Depletion of free charge carriers at junction between zones exhibiting deviating Fermi levels
  - *p*- and *n*-doped semiconductors
  - Metals
  - Insulators

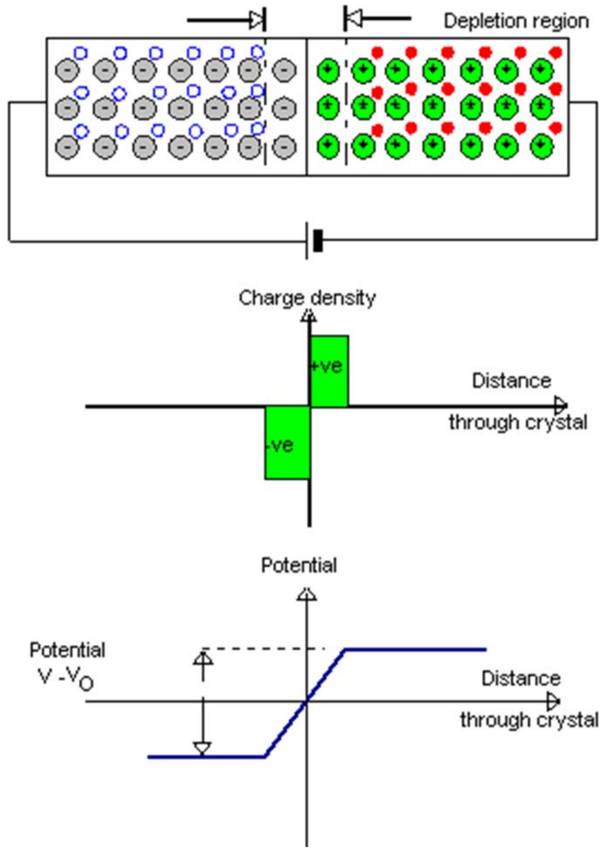

7.3.3. Chemdiodes

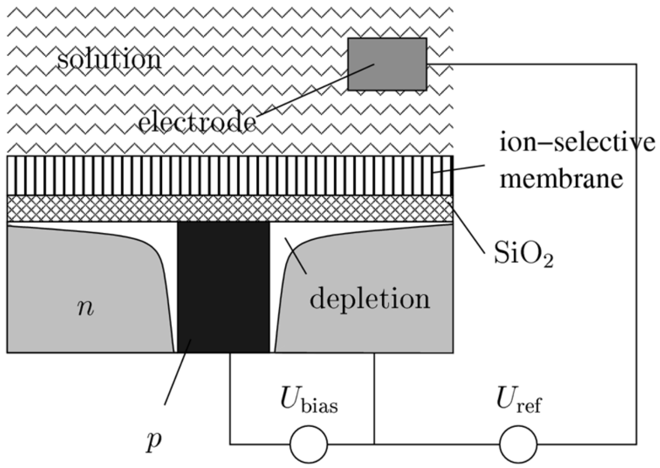

Fig. 7.4. Chemdiode

- Current across junction controlled by ion concentration of solution
- Horizontal *pn*-junction covered by silicon oxide layer
- Ion-selective membrane mediates contact between diode and solution
- Membrane may for instance be specific for hydronium or K^+ ions

7.3.3. Chemdiodes

- Voltage U_{ref} between reference electrode in solution and *n*-doped zone
- Bias voltage U_{bias} between *p*- and *n*-zone
- Reference voltage applied to generate depletion layer along *pn*-junction as well as SiO_2-*n*-Si interface
- Ion from solution penetrates selective membrane
  - ➢ Introduction of additional charge into depletion layer altering its thickness
- Capacitance of charge distribution across *pn*-junction changes according ion concentration of solution
- Magnitude of signal controllable by U_{bias}

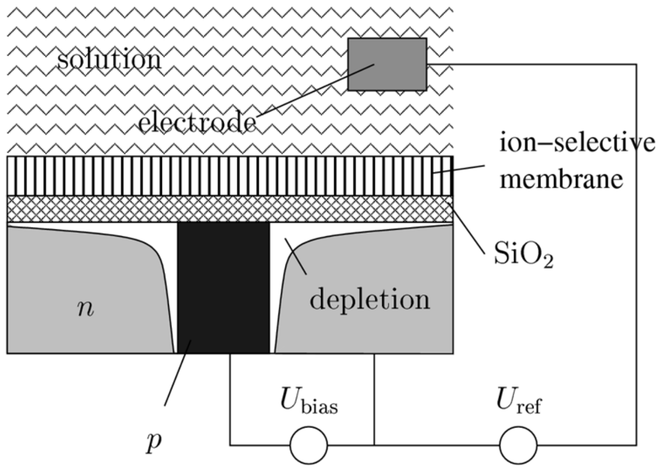

Fig. 7.4. Chemdiode

7.3.3. ADFETs, ISFETs and ChemFETs

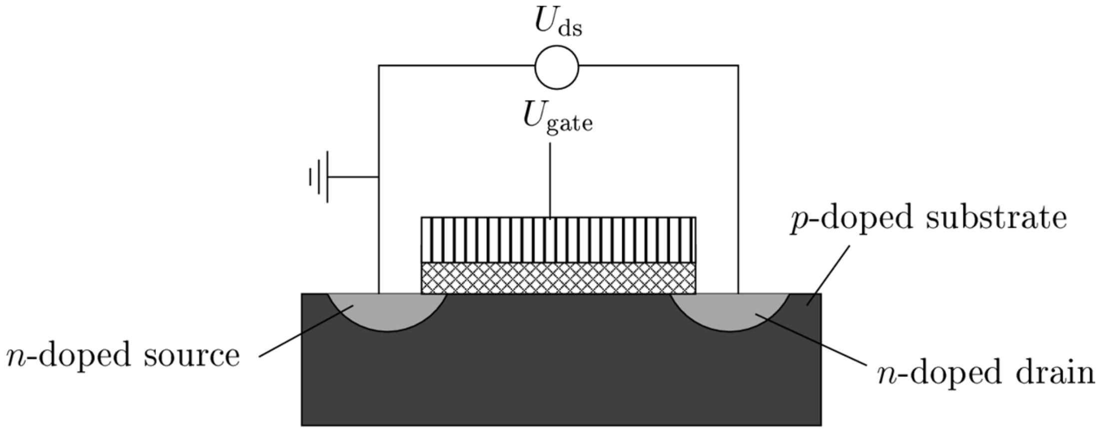

Fig. 7.5. Principle of a MOSFET (metal oxide field effect transistor). A depletion layer of free charge carriers forms at the interface between the p-doped substrate and the oxide due to the adjustment of the Fermi levels. According to the transistor principle, a small voltage $U_{\text{gate}} \ll U_{\text{ds}}$ controls the current between the n-doped source and drain by injection of charge carriers into the depletion zone

- MOSFET
  - Gate voltage controls current between source and drain electrode
- MOSFET principle for detection of atoms or ions
  - Removal of metal electrode layer
  - Usage of interaction of atoms, molecules and ions at the oxide surface as the gate voltage

7.3.3. ADFET

- Open-gate structure for gas detection
- Adsorption of polar molecules on oxide surface
  - Few nanometer thickness of oxide layer
- Molecules adsorbed on oxide layer impact current between source and drain
- High electric noise ratios due to open-gate layout
- Improvement for detection of hydrogen
  - Palladium (Pd) gate deposited upon oxide layer
  - Pd catalyzes dissociation of H_2 molecules
  - Atomic hydrogen (H) diffuses through Pd layer towards interface with oxide layer
  - Compared to „raw“ ADFET
    - Improved signal-to-noise level
    - Exclusion of atoms other than H from contact with oxide surface

7.3.3. ISFET

- Ion-selective FET
- Selective protonation / deprotonation of (mostly) pH-sensitive molecular layer at gate surface
- Surface charges built in response to pH of applied solution
  - ➢ Gating of current through transistor
- Detection of ions in solution in contact with oxide layer thus substitutes gate of MOSFET
- Chemical potential of ions depends on their concentration (activity)
- Ion concentration thus governs electrical properties of the FET

7.3.3. ChemFET

- Enabling detection of ions other than H^+
- Deposition of ion-selective membranes on surface of ISFET
  - Dip-coating or spinning ion-selective layer on oxide
- Additional layer
  - Either (electro-)chemically active for certain ion species
  - Or only distinguished ions pass through
- ChemFETs often basis for biosensors covered in next section

7.3.3. Metal-Oxide Gas Sensors

- Semiconducting metal oxide substrates acting as partial pressure sensors
- Electric conductivity significantly increases with temperature
  - ➢ Presence of point defects, e.g. interstitial atoms or voids, in semiconductor
  - ➢ Appreciable conductivity registered in range between 200-500°C
- Redox-reactions between gas molecules and point defect
  - ➢ Altering electric conductivity by removing or adding charge carriers
- Temperature also controls type of interaction between gas and substrate
  - ➢ Low temperatures
    - Physisorption via van-der-Waals bonds
  - ➢ High temperatures
    - Activation energy leads to strong ionic or covalent chemical bonds at surface and also within bulk
- Adsorbed molecules perform different redox-reactions with surface
  - ➢ Exchange of different numbers of electrons per reaction
- Efficiency of chemisorption
  - ➢ Peaks at deviating temperatures for different gas species
  - ➢ Supplying selectivity of sensor
- Large surface-to-volume ratios enhance sensitivity of sensor
- Common metal oxides
  - ➢ Alumina ceramics and silicon nitride

7.3.3. Pellistors

- Catalytic gas sensors
- Indirect detection of cases via rate of thermal energy released in exothermal reactions catalyzed at surface of sensor
  - ➢ Heating power proportional to reaction rate
  - ➢ Heating power proportional to partial pressure of gas
- Release of thermal energy picked up by temperature sensor
- Selectivity via choice of catalyst
- Pellistors usually operate at temperatures around 500°C
  - ➢ Small reaction rates of gases at room temperature

7.3. Chemical Sensors

1. Optical Detection
2. Electric Impedance Detection
3. Chemical Detection by Semiconductors
4. Biosensors

7.3.4. Biosensors

- Biosensors mostly based on ISFET concept
- Redox-system deposited on gate surface
- Immobilized biomolecules catalyze biomolecular redox-reactions
  - Altering pH-value and thus gate voltage
  - Example: NAD(P)+/NAD(P)H bio-catalysts
  - Immuno-sensitive FETs (IMFETs) so far rarely documented in literature
- Problems
  - Sensitive bio-electronic/biochemical transducer surfaces often not stable
  - Signal drifts with time
  - Non-specifically generated signals generate background noise
    - E.g. by other constituents of sample
  - Surface sensitive biosensors normally need fluidic control for continuous calibration or differential measurement with control liquid